Thermal Recovery Design to Improve the Efficiency of a Small-Scale Compressed-Air Energy Storage (CAES) System

A Major Qualifying Project

Submitted to the Faculty of

WORCESTER POLYTECHNIC INSTITUTE

Authors:

Meghan Brady

Dylan Connors

Mikaela Drake

Taylor Nowak

Maureen Ye

Date:

March 25th, 2022

Acknowledgements

We would like to thank those that have helped us throughout the course of this project and gave us the resources to achieve our final results. Firstly, we would like to thank Barbara Furhman for ordering all of our necessary parts and being very accommodating when we needed to special order items from various vendors. We would also like to thank Peter Hefti for his help in lending us specific materials and electrical testers from his personal office and providing storage and space for us to work. Lastly, we would like to thank our advisor, Professor Brian Savilonis for his invaluable guidance throughout all stages of our project.

Abstract

Efficient energy storage bridges the divide between supply and demand. One method of energy storage is compressed air energy storage (CAES) systems, which is currently only used on a large scale. The goal of this project was to build a thermally efficient CAES system for a small-scale application. Our final system extracts energy in the form of latent heat by using a water coil heat exchanger. Our system raised 10 L of water an average of 6.5 ºC and reached a maximum system output of 8.92 V. We evaluated the power output of the system, supported by theoretical analysis and experimental research. Future recommendations explore using a different energy extraction system to maximize power output and changing standard pressures and sizes of system materials to generate improved results. The flexibility and environmental friendliness of this system emphasizes the potential of small scale CAES systems in the future.

Authorship

Section	Primary Author(s)	Primary Editor(s)
Abstract	Meghan Brady; Mikaela Drake	Taylor Nowak
Executive Summary	Meghan Brady: Mikaela Drake	
1.0 Introduction	Mikaela Drake; Taylor Nowak	
2.0 Background		
2.1 Types of Energy Storage		
2.1.1 Batteries	Mikaela Drake	Maureen Ye
2.1.2 Flywheels	Dylan Connors	
2.2 Compressed Air Energy Storage		
2.2.1 Large-Scale CAES	Meghan Brady	Taylor Nowak
2.2.2 Small-Scale CAES	Mikaela Drake	Taylor Nowak
2.3 Improving Efficiency in CAES	Dylan Connors	
2.3.1 High and Low Pressure Systems	Mikaela Drake	
2.3.2. Isentropic Compression	Meghan Brady, Taylor Nowak	
2.3.3. Isothermal Compression	Meghan Brady, Taylor Nowak	
2.4 Thermal Recovery and Phase Change Materials	Mikaela Drake	
2.5 CAES Regulations	Mikaela Drake	
3.0 Theoretical Design		
3.1 Proposed CAES Systems	Mikaela Drake	
3.2 Material Selection	Dylan Connors	Mikaela Drake
3.3 Preliminary Thermodynamic Analysis	Meghan Brady; Taylor Nowak	
3.3.1 Isentropic Compression Analysis	Meghan Brady; Taylor Nowak	
3.3.2 Isentropic Expansion Analysis	Meghan Brady; Taylor Nowak	
3.3.3 Isothermal Compression Analysis	Taylor Nowak	
3.4 Storage Tank Theoretical Analysis	Taylor Nowak	Meghan Brady; Dylan Connors
3.4.1 Tank Filling	Taylor Nowak	Dylan Connors
3.4.2 Tank Emptying	Taylor Nowak	Meghan Brady; Dylan Connors

3.5 Heat Loss and Insulation		
3.5.1 Thermal Resistance	Mikaela Drake; Maureen Ye	Meghan Brady; Dylan Connors
3.5.2 Insulation	Meghan Brady; Dylan Connors; Taylor Nowak	Dylan Connors
3.5.3 Heat Loss Over Time	Meghan Brady; Taylor Nowak	Dylan Connors
4.0 Methods		
4.1 Basic System Testing	Taylor Nowak	Meghan Brady
4.1.1 Testing Procedure	Dylan Connors	Meghan Brady
4.1.2 Results and Analysis	Mikaela Drake; Taylor Nowak	Meghan Brady
4.2 Motor and Drill Mounting	Dylan Connors	Meghan Brady; Mikaela Drake
4.3 Heat Exchanger Design (Meghan)		
4.3.1 Theoretical Analysis	Taylor Nowak	Meghan Brady; Dylan Connors
4.3.2 Copper Piping Selection and Analysis	Dylan Connors; Taylor Nowak	Meghan Brady; Dylan Connors
4.3.3 Heat Exchanger Build	Maureen Ye	Meghan Brady; Dylan Connors
4.3.4 Final System Build	Dylan Connors	Meghan Brady; Dylan Connors
4.3.5 Electrical Impedance	Mikaela Drake	Meghan Brady; Dylan Connors
4.3.6 Final System Testing Procedure	Dylan Connors; Mikaela Drake	Meghan Brady
5.0 Results and Analysis		
5.1 Heat Exchanger Results	Taylor Nowak	Meghan Brady
5.2 Discussion	Mikaela Drake	Dylan Connors; Maureen Ye
6.0 Conclusions and Recommendations		
6.1 Recommendations for Future Work	Mikaela Drake	Taylor Nowak; Maureen Ye
6.2 Conclusions	Mikaela Drake	Meghan Brady; Maureen Ye
Appendices	All	All

Table of Contents

List of Tables

List of Figures

Executive Summary

Energy storage is key to creating a more accessible energy system, as the need for energy storage is a growing concern due to the negative environmental impact of fossil fuels. An increased effort to find solutions within the realm of renewable resources has hit the issue of intermittency problems and unpredictable conditions. Electrical energy storage (EES) is the sector that is attempting to overcome this problem using batteries, flywheels, compressed air, and less commonly hydro pumped generation, molten salt (thermal) generation, and hydrogen systems. Batteries are the most common storage systems used; however, they have a maximum number of cycles. Alternatively, compressed air energy storage systems have a lifetime of up to 40 years.

Energy storage is key to creating a more accessible energy system, as the need for energy storage is a growing concern because of the negative environmental impact of fossil fuels. An increased effort to find solutions within the realm of renewable resources has hit the issue of intermittency problems and unpredictable conditions. Electrical energy storage (EES) is the sector that is attempting to overcome this problem using batteries, flywheels, compressed air, and less commonly hydro pumped generation, molten salt (thermal) generation, and hydrogen systems. Batteries are the most common storage systems used; however, they have a maximum number of cycles. Alternatively, compressed air energy storage systems have a lifetime of up to 40 years.

Battery storage systems (BSS) are commonly used to maintain independent power grids; however, they have become more expensive than other sources of energy storage due to the cost of frequency regulation. The most common batteries used are lithium-ion batteries due to their stability and the fact that they have been heavily tested. Batteries pose safety and environmental issues, as they can catch fire if not properly maintained and need to be properly disposed of. Another form of energy storage is compressed air energy storage (CAES) systems, where energy is stored in the form of compressed air.

Typically, CAES systems perform on a commercial scale where air is stored in large caverns and generate energy when air is passed through a turbine. This is useful because it allows a reserve of energy to be held without the need of an external energy source like wind or solar power requires. CAES systems can produce around 100-300 MW over long-term periods, showing that these long-term systems are very applicable and versatile. term systems are very applicable and versatile. They do not produce harmful waste and have a fast startup time of about 30 seconds.

Even though CAES systems have immense potential, there is minimal work or research completed on the small-scale application of CAES systems. Small-scale systems typically store energy with the kW range, compared to MW for large-scale systems, making them less efficient because there is less available energy to recover during the compression stage. To implement a small-scale CAES system in an application such as an apartment, architectural and structural planning of either the building or the tank is needed which is much more expensive upfront.

Improving the efficiency of a CAES system is the main goal of this project. The low efficiency of many large-scale CAES systems is due to the direct heat loss from the compression of air. To improve the efficiency of the overall CAES system (at both large and small-scale) the heat losses need to be recovered or recycled. To achieve this, our team built an external heat exchanger to extract latent heat between the compression and storage stages and store it as energy.

Initially we focused on three iterations that each used different methods of energy to increase system efficiency: an insulated system, a cogeneration system, and a system using thermal storage. The simplest CAES system does not have any of these additions and consists only of an air compressor, storage tank, and turbine. The second iteration adds insulation to the air tank to decrease the heat loss leaving the tank. As a result, the temperature of the air stored in the tank theoretically stays hot for longer. The next iteration integrates a heat exchanger to be used in conjunction with another power system where the heat from compression is used to heat an area of a room or power an external appliance. While this does not directly improve the internal system efficiency, this approach maximizes the amount of energy of the system overall. The final iteration of the basic CAES system introduces a thermal energy storage unit. This thermal storage system presents many similarities to the cogeneration system. However, the extracted heat during compression is not used outside of the system but is later reintroduced into the system before the air enters the turbine. We completed theoretical analyses of all four different systems, calculating the maximum temperatures reached and the maximum efficiencies achieved.

Due to external factors, we decided to conduct experiments on the baseline CAES system with no added features, and on a system with an external heat exchanger. In order to complete testing on this second system we built a heat exchanger using copper piping and a cooler to store water. The original pipe connecting the compressor and the tank was cut to fit the copper piping at the top of the heat exchanger. We covered the piping with fiberglass insulation to minimize the heat loss. We connected the outlet of the heat exchanger to the inlet of the tank. We used Teflon tape at all these connections for a tighter seal.

Our testing began with the baseline CAES system consisting only of an air compressor, storage tank, and turbine. The tests involved tank emptying and filling, where we measured the time, it took for the tank to fill to 1379 kPag (200 psig), the mass added to the system, and the temperature of the air. During filling we measured the temperature of compressed air every 30 seconds using a thermocouple held to a predetermined spot on the metal pipe connecting the compressor to the tank. To conduct tank emptying experiments we let the air out through the drill connected to the tank through an impact hose. To predict the amount of thermal energy lost over time, our team measured the rough temperature at both the top and bottom of the outside of the tank every five minutes for a total of forty minutes. We also tested the voltage output of the entire system.

The testing of our heat exchanger system involved timing how long it took to fill, the temperature of the water, time to empty, and the voltage produced. To begin testing, the heat exchanger was filled with 10 L of room temperature water and was placed on a leveling table to raise it to a proper height for connection to the compressor. The heat exchanger outlet was then connected to the air tank using the rubber hose and the thermocouple measured the starting temperature of the water. The compressor was turned on and temperature measurements of the water were taken in 60 seconds intervals, as well as the time to fill. When emptying, the air drill allowed complete continuous emptying and the instantaneous voltage was recorded every 30 seconds, as well as total time to empty. The heat exchanger system raised 10 L of water an average of 6.5 ºC and reached a maximum output of 8.92 V. While the maximum voltage wasn’t as high as we were hoping, our team was able to save roughly 300 kJ of energy in the water. With a higher pressure and a larger system, this captured thermal energy could easily be turned into usable power, such as in a water heater.

Our team achieved our original project goal to build and test a working model of a compressed air energy system with a working heat exchanger. Over the 21 working weeks, our project took many different forms using different methods of thermal energy recovery, different materials, and different standard values. As our team designed and developed this project, many preliminary goals and objectives became unrealistic with the time and resources available. However, we fully believe that this project has a lot of potential in the research for small-scale

CAES systems. By changing different parts of our system (such as the amount of water, size of storage tank, type of heat exchanger material, etc.), this project can be replicated to get very different, and perhaps better, results.

1.0 Introduction

1.1 The Demand for Energy Storage

Energy storage is the key to creating more widespread, accessible, and flexible energy systems; it is the bridge between the availability of energy and its demand. The need for energy storage parallels the growing concern regarding the environmental impact of fossil fuels. Recent studies show that almost 70% of global electricity generation is due to the use of fossil fuels [1]. With a higher need for renewable energy sources and growing respect for the environment, efforts have been made to find greener solutions. However, renewable energy solutions such as wind and solar remain inconsistent energy sources due to their intermittency and sometimes unpredictable conditions [2]. Electrical energy storage (EES) aims to balance the need between supply and demand, storing energy to be used in off-peak times [1]. Common energy storage solutions include batteries, flywheels, and compressed air.

Currently, CAES systems are large-scale operations used with energy sources, such as gas or oil. There is a current technology gap in the development of CAES systems for the small-scale uses, like that of an apartment or house. These small-scale systems have the potential to provide energy during off-peak times, when solar or wind electric generating systems are nonproductive. Compressed air energy storage presents the challenge of conserving thermal energy produced during the air compression process. The goal of this project was to improve the efficiency of small-scale CAES systems through the design of a cogeneration system and evaluate the application of small-scale storage systems for a home or apartment to help solve the energy storage issue of the future.

To complete this goal, we completed the following objectives:

1. Gain a baseline understanding of current CAES technology.
2. Determine type of system to build and select components for the system.
3. Perform a preliminary theoretical analysis of air compression cycle and thermal exchanges.
4. Conduct preliminary testing to compare theoretical (expected) results to experimental results.
5. Design and build a working prototype to examine and optimize thermal efficiency of the overall system.

6. Conduct testing of thermal storage device working in conjunction with small scale CAES system.
7. Analyze results to determine effectiveness of thermal storage device.

2.0 Background

In this section, we provide relevant background information detailing types of energy storage. As compressed air energy storage (CAES) is the focus of this project, we further detail different types of CAES systems that aim to improve system efficiency, as well as current CAES regulations.

2.1 Types of Energy Storage

There are many types of energy storage solutions. Common energy storage solutions include batteries, flywheels, and compressed air. Less common systems include hydro-pumped generation, molten salt (thermal) generation, and hydrogen. Table 1 outlines some of the key characteristics of the common energy storage technologies [2].

Table 1: Characteristics of energy storage systems

Type of Storage	*Max Power Rating (MW)*	*Discharge Time*	*Lifetime (years)*	*Energy Density (W/L)*	*Efficiency*
Compressed air	1000	2-30 hours	20-40	2-6	40-70%
Li-ion battery	100	1 min- 8 hours	1,000- 10,000	200-400	85-95%
Flywheels	20	seconds- minutes	20,000- 100,000	20-80	70-95%

As detailed in Table 1, the most efficient energy storage is generally batteries, typically achieving almost 90% efficiency [2]. The tradeoff with batteries is their max cycles; batteries have a maximum number of cycles, while other energy storage technologies, like compressed air, have a total lifetime of 20-40 years [2]. While batteries and flywheel storage appear to have more benefits in almost all categories, a deeper look into the environmental and economic backgrounds of each type of storage is needed to provide a better understanding of energy storage technologies.

2.1.1 Batteries

Battery storage systems (BSS) are a reliable and stable method of energy storage. BSS are commonly used to maintain independent power grids that are less stable when maintaining a constant voltage. While BSS have been studied and well understood, they have become more expensive than other sources of energy storage, most due to the cost of frequency regulation [3]. However, BSS are increasing in popularity with the development of electric cars.

The most common battery used is the lithium battery, due to its stability in both residential and commercial settings. While it is safest and most thoroughly tested option, all batteries can pose danger if not maintained. Lithium-ion batteries have been known to catch fire and fail in a process called thermal runaway; this is dangerous if not controlled or expected. Another issue following battery storage is its environmental impact. Batteries have been applied to renewable energy sources, such as solar panels, to store energy for cloudy days. However, batteries cannot last forever, and the waste product is difficult to properly dispose of. Battery storage can present environmental hazards if the raw materials, like lithium and lead, are not disposed of properly [4]. Most batteries are broken down into their individual parts and reused separately. While BSS is currently the most popular form of energy storage, especially at small-scale levels, other energy storage systems options have a lesser impact on the environment and are more cost-effective [3].

2.1.2 Flywheels

Another popular energy storage solution are flywheels, which can sometimes be referred to as a mechanical battery. Flywheel energy storage consists of a balanced disk rotating at high speeds. The rotational energy stored in this device is converted into electrical energy through the engagement of an electrical generator, such as an alternator. The rotating disk, the flywheel, is mounted in a mechanism that maintains the position of the flywheel to minimize any friction. In more complex flywheel batteries, the mechanism is placed in a vacuum, and magnets are used to suspend the flywheel to eliminate friction from the air and any contact points. These flywheels can rotate at speeds upwards of 50,000 revolutions per minute (RPM). Standard flywheels use metal bearings and are less efficient. The mass and RPM of the flywheel determine the stored kinetic energy that is transferred into electrical energy. Energy from renewable sources spins the flywheel to the desired RPM. In times of high demand, power is drawn from the kinetic energy of the rotating flywheel [8].

2.2 Compressed Air Energy Storage

Another form of energy storage is compressed air energy storage (CAES) systems, where energy is stored in the form of compressed air. Air is compressed, typically with a rotary compressor, and stored in an air storage tank or system until usage. Typically, CAES systems are on the commercial scale. In these larger applications, compressed air is often stored in caverns, while in smaller applications, air is stored in portable air tanks. When energy is needed, the air stored in either a cavern or tank is passed through an air turbine to then generate energy. Standard CAES plants have lower efficiency than newer and more advanced CAES systems like adiabatic and isothermal CAES, that seek to improve system efficiency [5].

CAES systems are used to restore electric power stations or parts of a grid without using an external energy source. These systems are capable of running independently due to their ability to store an unused capacity of energy assets called a "spinning reserve" [11]. In some cases, the power stored in the reserve is generated from a separate energy system and used only during power outages. This is a common responsibility of CAES in smaller energy systems. While the integration of CAES is not widely used, there are many potentials uses for applications in development.

There are currently only two operating CAES plants globally: a 110 MW plant in Alabama and a 290 MW plant in Germany [6]. The small-scale CAES system is a newer concept, as the first study on small-scale CAES was published in 2010, and there are no commercial products currently available [7].

CAES provides a large-scale economical grid-scale solution. There is minimal work and research completed on the small-scale application of CAES systems. Flywheel storage systems can produce high power (100 kW to 2 MW) for a short amount of time, around 12-60 seconds, while CAES systems produce around 100-300 MW for days [8]. For long-term storage, CAES systems are more applicable and versatile. CAES systems compress air from the surrounding environment and do not produce harmful waste. Another advantage of CAES systems is that it has a fast startup time, about 30 seconds; a smaller scale plant could respond in 10 seconds [9]. Flywheel energy storage has an even faster response and startup time than CAES but due to its short run time, it is not feasible in specific applications. From an economic perspective, CAES is relatively cheap, at $400-500/kW [10].

2.2.1 Large-Scale CAES

Large-scale CAES has been around for over 40 years, though it has few large applications in present power systems. Large-scale CAES facilities store large quantities of energy, currently up to 300 MW, for 48 hours, far exceeding lithium-ion batteries storage capabilities [15]. In recent years, lithium-ion batteries have made major improvements, though CAES systems show much more potential in becoming more cost and environmentally efficient for large-scale energy operations.

Large-scale CAES plants store compressed air in underground caverns. In times of peak power production, a large-scale water-cooled compressor is used to pump compressed air into the underground cavern. These caverns are either man-made or empty salt caverns. When the grid requires power, the compressed air is released through a pipe directly, feeding a turbine. Before the air enters the turbine, small amounts of natural gas are used to heat the pressurized air to increase the efficiency of the turbine. In more efficient CAES plants, the heat produced from the compressor during the filling period is stored in a separate thermally isolated loop. This energy is stored in the form of heated water or other fluids. The stored heat is then re-introduced through a heat exchanger before the air enters the turbine [10].

2.2.2 Small-Scale CAES

Compared to large-scale systems, there is significantly less research on the application of small-scale CAES technology. Small-scale CAES systems store much less energy, typically within the kW range, compared to MW for large-scale systems. This difference in energy is partially due to smaller systems being generally less efficient, as the amount of access to small-scale energy recovery systems is smaller. The smaller amount of space within the system limits the ability to recover any energy lost during the compression stage, as there is less energy [7]. One example of a working small-scale application of CAES is found in the EU, where they prototype photovoltaic (PV)-CAES system to power older historical buildings. This system design matched the space and architectural demands of the building location; the system met 26% of the demand of the building [7]. This study supports the adaptability of CAES systems to smaller environments, based on individual needs.

When comparing small-scale and large-scale CAES systems, large-scale CAES plants are more inefficient compared to hydropower plants or chemical batteries [7]. However, many researchers have been looking into the small-scale, or microsystems, of CAES for household purposes. Similar to chemical batteries, micro-CAES can be built virtually anywhere, as demonstrated in the EU prototype discussed above. On small and large scales alike, CAES is a cleaner, renewable, longer-lasting solution to energy storage and generation.

The main drawback with small-scale CAES is the same as large-scale: finding available space for the storage vessels and the system. While this challenge is avoided through architectural and structural planning of either the building or the tank, this is much more expensive upfront. The general lower efficiency of CAES poses an issue as well, as the size of the storage vessel and efficiency of the system go hand-in-hand. Increasing the storage pressure minimizes the volume needed, however, this decreases the efficiency of the system [16].

2.3 Improving Efficiency of CAES Systems

Improving the efficiency of CAES systems is at the forefront of CAES technology. The low efficiency of many large-scale CAES systems is due to the direct heat loss from the compression of air. To improve the efficiency of the overall CAES system (at both large and small-scale) the heat loss is recovered or recycled [7]. Current technology is looking at ways to improve the overall efficiency of the system.

2.3.1 High and Low-Pressure Systems

Currently, two main strategies are being researched in the development of micro-CAES systems: low pressure and high-pressure systems. These two low-tech methods are vastly different from those used for larger systems. Low pressures are used to keep the temperatures at compression and expansion roughly the same, to limit any thermal energy loss. The high-pressure systems are designed specifically for household applications like heating and air conditioning.

In high-pressure systems, the heat loss during compression is used to power household applications. In this design, the inefficiency of the system is harvested as thermal power and repurposed to other systems, such as heating water or generating electrical energy. This is an advantage over chemical batteries and increases the all-over efficiency of the system from around 45% to 80% [16]. This system can supply heat and cooling systems, therefore, some appliances are deemed unnecessary, such as air conditioning or electric boilers. Another benefit of high-pressure systems is the limit of storage size. With higher compression, more air, and therefore more power, can fit within a smaller storage vessel. This makes high-pressure systems ideal for small-scale residential buildings. The largest disadvantage of this system is the need for more expensive storage tanks, and some extra space for heat exchangers.

In low-pressure systems, the goal is to make the system as near-isothermal as possible. This is completed by lowering the storage pressure of tanks below 10 bar, where the air exhibits an extremely low-temperature change during expansion or compression. With such a small temperature change, the efficiency of the system can reach nearly 100%.

2.3.2 Isentropic Compression

Isentropic compression is an adiabatic process in where there is no heat transfer between the system and the environment; entropy remains constant. In an Adiabatic-CAES (A-CAES) system, the thermal energy generated from the compression stage is stored and put back into the system when the air is released, heating the air before passing it through a turbine. This removes the need for outsourcing heat in this stage [5]. Adiabatic systems can achieve a much higher efficiency than the standard CAES system. Adiabatic systems can achieve up to 70% efficiency if the heat waste from compressed air is covered and then used to re-heat the compressed air during the turbine stage [17].

There are two types of A-CAES systems: A-CAES without Thermal Energy Storage (TES) and A-CAES with TES. In A-CAES without TES, the air is not cooled after each compression stage and instead it is stored at higher temperatures, removing the need to heat the air after releasing it. Although thermal energy loss is reduced, this system has significant disadvantages. Due to the high temperatures, the air cannot be compressed at high pressures. This reduces the potential for storing energy and increases the price of the storage vessels needed for higher temperatures. A-CAES with TES is a more viable option because thermal energy storage is used. Heat is removed from the air after compression and stored in an appropriate storage medium. The stored heat is then used to heat the air before it goes through the turbine. This type of CAES system reaches about 75% efficiency. However, a drawback of this system is the cost [5].

2.3.3. *Isothermal Compression*

An isothermal CAES (I-CAES) system keeps the air at a constant or near-constant temperature throughout the entire process. The power required to run the compressor is less than an A-CAES to maintain the same pressure ratios. Heat is removed from the air during compression and reintroduced during expansion. While this sounds similar to A-CAES, the key difference is that in I-CAES, heat is continuously removed during compression and added during expansion keeping the temperature constant, whereas in A-CAES, the heat is added or removed after each compression or expansion stage and the heat is stored. One advantage to I-CAES is that it could have an efficiency of around 80%. However, it is still in the early research phase and there are still issues with keeping the system at a constant temperature [5].

2.4 Thermal Recovery

One of the key issues small-scale CAES faces is the lack of thermal energy created. Since the micro-CAES generates less energy, there is less heat generated. In return, there is less heat to extract and reintroduce into the system. There is limited research done on thermal storage for micro-CAES. Most often, the excess heat is used to heat a room directly, or the cooled air is used to moderate the temperature of a refrigerator. Finding new ways to incorporate different types of thermal storage is the next step in the development of household CAES [18]. The typical American 1–2 bedroom apartment uses 20-30 kWh total energy per day [25]. The design of a small-scale CAES system must consider this daily energy usage.

Thermal storage is an additional application that is currently added onto large-scale CAES plants to increase the efficiency of the systems. These heat transfer systems typically use a large radiator and piping with a flowing cooling liquid (often water), heating and cooling the compressed air at different stages of power generation. The heat transfer system cools the air leaving the compressor before it is stored and heating the air before it is expanded. This results in an overall increase in system efficiency because less energy is wasted as ambient heat during the compression stage [18].

2.5 Compressed Air Energy Systems Regulations

CAES systems remain a relatively new concept for electrical energy storage, and most of the current research and implementation is completed on the large scale. Many state regulations for CAES systems in the United States apply to the construction and changes made to existing or new power plants. Small-scale systems are not as common, and most of the restrictions that apply to their introduction into homes come from construction liability standards and water/oil acquisition [19]. The focus for regulating CAES systems comes at a federal level and focuses on issues, including environmental regulations, liability rights, and property rights. Since there are not as many household systems, there is less attention given to regulatory issues on state or local levels [19].

For many CAES systems, water is commonly used within the heat transfer process for cooling at different parts of the cycle. In any situation where water is used within a system, regulations under the Clean Water Act (CWA) must be met [19]. Where the water is taken from, how it is used, and how it exits the system are all factors of CAES systems that fall under surface water quality control and require pollution restriction permits, such as a National Pollution Discharge Elimination Permit (NPDES) [19]. Almost all states require permits regulating the use of surface and underground water and how much is used and affected during cooling processes.

Under the same category, if oil is used anywhere in the system, like during compression, there are federal and state oil storage regulations that are in place to prevent any oil runoff into ground or surface water reservoirs. While there is research currently being completed on CAES systems that eliminate the need or use for oil, there is still a long way to go until oil-free CAES is developed. Until then, any implementation of these systems must abide by oil storage and disposal regulations [19].

3.0 Theoretical Design

In order to achieve our project goal of improving the efficiency of small-scale systems, we began with a theoretical design of a small-scale system. Throughout our research on current models of small-scale CAES systems, our team determined a major drawback of current models of small-scale CAES systems is the low energy efficiencies of the systems. Additionally, there is the current gap in models of small-scale CAES. Our theoretical design began by drafting a basic CAES system and three iterations that each use different methods of energy to increase system efficiency. The types of CAES systems include a basic system, an insulated system, a cogeneration system, and a system using thermal storage. Next, we used our basic system to aid in selecting our key materials: a compressor, an air tank, and a turbine. We performed preliminary theoretical calculations to determine the temperatures and pressures at various locations in our system. Lastly, we validated these calculations with preliminary testing to compare our theoretical results with our experimental data.

3.1 Proposed CAES Systems

3.1.1 Simple CAES System

Figure 1 below depicts the simplest CAES system. The three main components of the system are the air compressor, storage tank, and turbine; these three components are standard in the other variations of CAES systems detailed below as well. In the basic system, air enters the compressor, is stored in a storage tank, and expanded through a turbine. This system represents the most basic skeleton version of a small-scale system. All system analyses assume standard temperature and pressure conditions for the inlet air, 293K and 101 kPa.

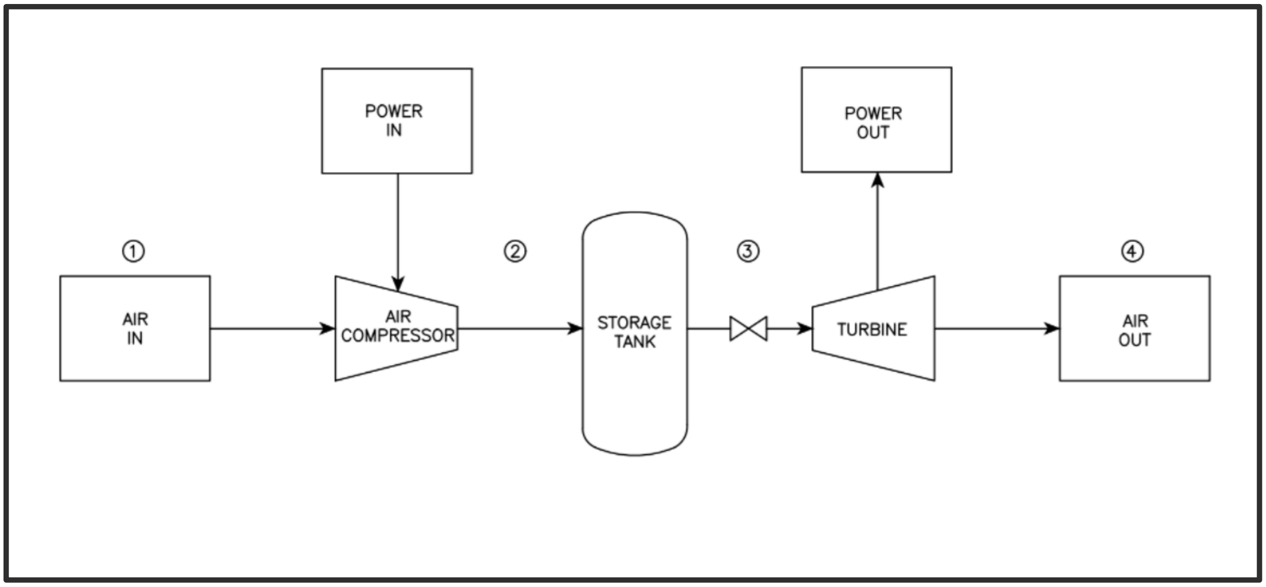

Figure 1: Simple CAES system

3.1.2 Insulated System

The first iteration of the basic CAES system requires an insulated air storage tank. As depicted below in Figure 2, the only difference between the basic system and this iteration is the insulated storage tank. As the air moves through the compressor, the air is compressed, thus increasing the temperature of the air. As a result, the temperature of the air leaving the compressor and entering the storage tank is greater than the inlet temperature of 293K. However, there is heat loss in the storage tank as the hotter air sits in the tank. The insulated systems aim to minimize the heat loss in the storage tank.

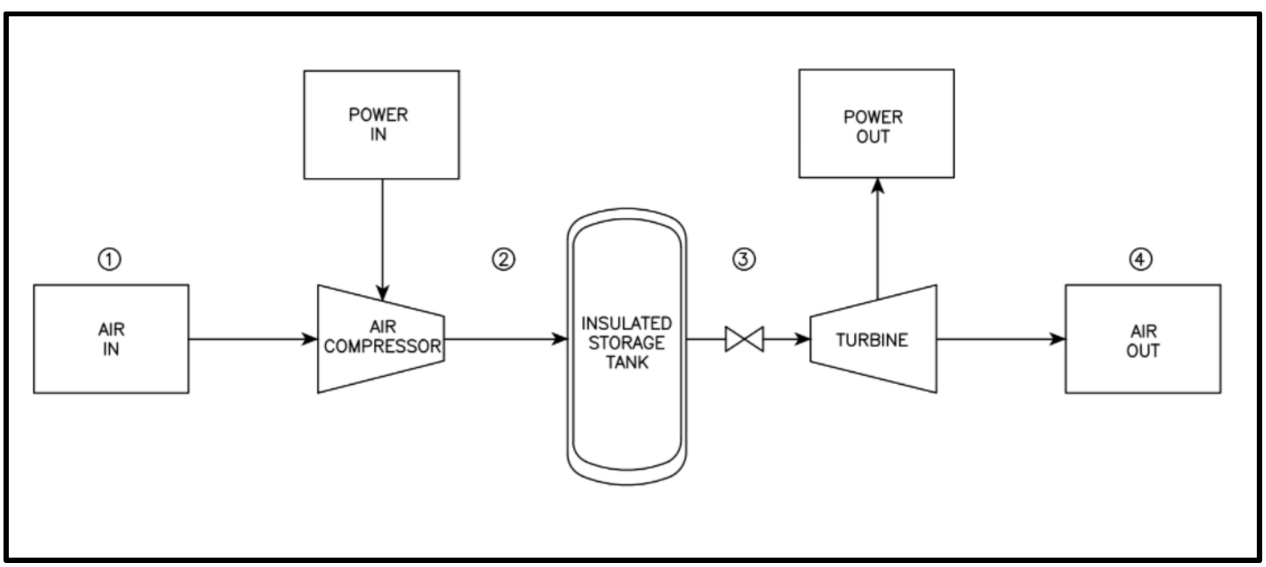

Figure 2: Insulated CAES system

3.1.3 Cogeneration System

The second iteration of the basic CAES system requires an additional component to the system: a heat exchanger. Small-scale CAES systems are used in households, in conjunction with another power system. This is known as a cogeneration system. In this system, the heat extracted from compression is used outside of the CAES system. Examples of uses of the extracted heat include hot water tank or other heating applications. While this does not directly improve the internal system efficiency, this system maximizes the amount of energy of the system overall. This results in two sources of power: the external appliance and the turbine.

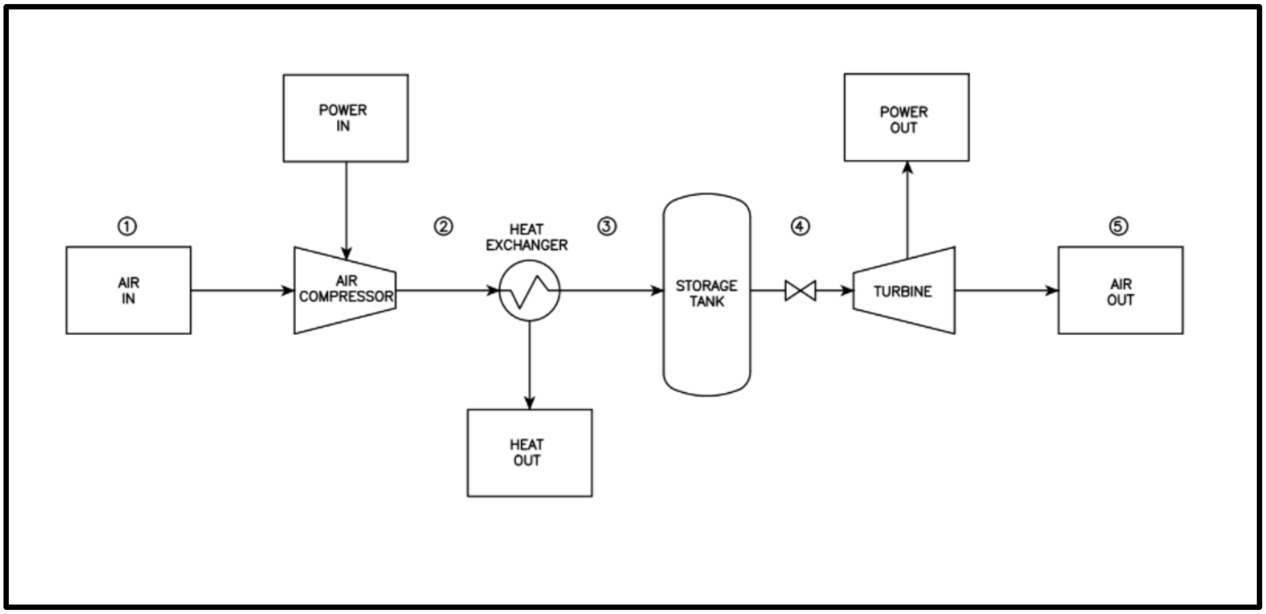

Figure 3: Cogeneration CAES system

3.1.4 Thermal Storage System

The final iteration of the basic CAES system introduces a thermal energy storage unit. This thermal storage system presents many similarities to the cogeneration system. However, the extracted heat during compression is not used outside of the system but is later reintroduced into the system before the air enters the turbine. This thermal energy storage system cools the air before it is stored and allows the tank to hold a higher volume of air. This results in the greatest energy output before the turbine. The process of storing energy, though still within our system, can increase the internal efficiency of the system and maximize the energy output. While investigating this system, we assumed the heat exchanger could extract all the heat during compression, store it over time, and completely reintroduce it back into the system.

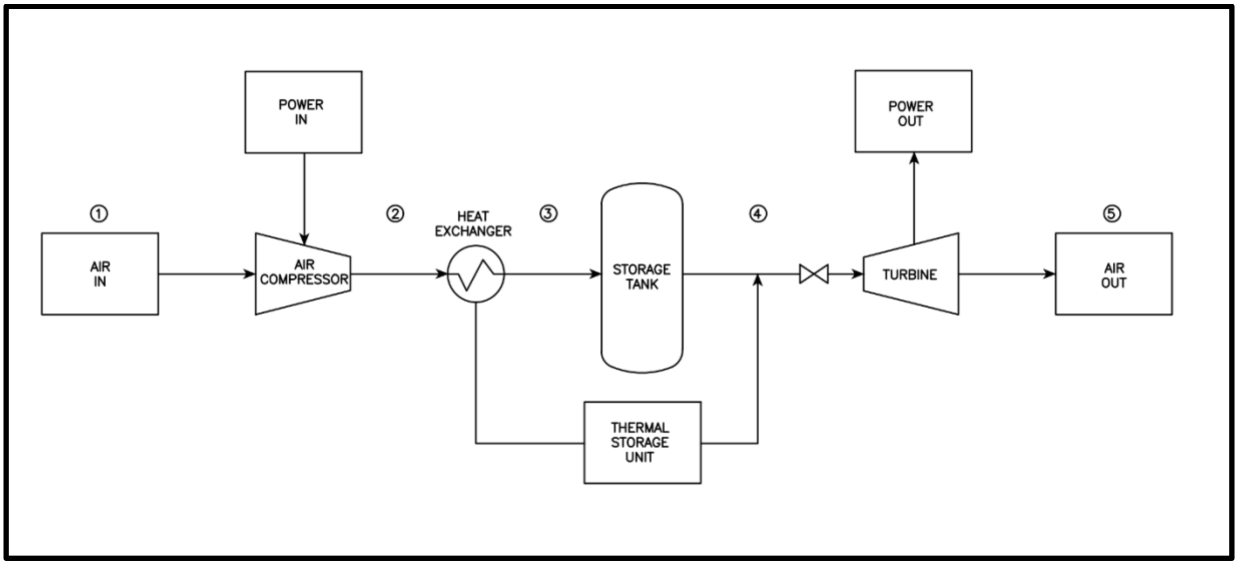

Figure 4: CAES system with thermal storage unit

3.2 Material Selection

Experimental small-scale CAES systems still present technical complexity in their design and operation. The design of our experimental setup required preliminary calculations to aid us in selecting an appropriate air tank and compressor for our small-scale application. First, we calculated the total available energy from different sizes of compressed air tanks. This analysis indicated the total energy in watts, that we could store and convert to electrical energy.

The analysis below determined the potential energy of the compressed air or the theoretical kWh output for each tank configuration. The results of the analysis are detailed in Table 2. This preliminary analysis allowed our team to determine the appropriate tank size and specifications.

Table 2 details tank volume in both gallons and m^3. Gallons are the specifications provided from the manufacturer, while m^3 are used in the calculations. Similarly, pressure is provided in both psi and kPa. Psi is again provided from the manufacturer while kPa is used in the analysis. Throughout future analyses, both units will be presented for clarity.

The maximum work of the tank is defined as:

$$W = \frac{V \times c_v \times (P_2 - P_1)}{R} \tag{1}$$

Where:

W=work [kJ]

V=volume of the tank [m^3]

c_V= specific heat at constant volume = 0.718 [kJ/kg K]

R= universal gas constant= 0.287 [kJ/kg K]

P_1= inlet pressure (constant) = 101 [kPa]

P_2= maximum pressure of the storage tank [kPa]

Table 2: Air Tank Sizing Comparison

	Option 1	**Option 2**	**Option 3**
Tank Volume (gal)	*20*	*5.0*	*3.0*
Tank Volume (m^3)	0.08	0.02	0.01
Maximum Tank Pressure_ P_2 (psig)	*200*	*150*	*3,000*
Maximum Tank Pressure_ P_2 (kPa)	1,379	1,034	20,684
Max Work of Tank (kJ)	242	44.2	584
kWh	**0.07**	**0.01**	**0.16**

Following this analysis, we selected Option 1 for our storage tank and air compressor. This option balanced tank size, of 20 gallons, and maximum pressure, of 200 psig. Our team's selected components for the small-scale CAES build are detailed below in Table 3. The 3000 psig scuba tank provided the largest potential energy. However, the cost and complexity of the compressor and the corresponding fittings made this option out of reach. Within our maximum budget of $1,250, the 20-gallon 200 psig tank provides adequate thermal and potential energy. The fittings and piping associated with this tank were also readily available and simplistic. To convert the stored compressed air into rotational mechanical energy, we selected a turbine compatible with the pressure and CFM available from the chosen tank. To ensure compatibility, we selected an air drill, acting as the turbine, designed to use with the selected tank. The air drill is specified to run at 2000 RPM with a 90 psig flow of compressed air, at 3.6 cubic feet per minute. Some lubrication is required to reduce the friction within the turbine.

To convert this rotational energy to electrical energy, we selected a DC motor capable of running in reverse at the expected RPM of the air drill. The reverse rotation of the DC motor produces an electric charge in 12 volts. Frictional losses are minimized as the DC generator is directly driven by the turbine. To prevent mechanical vibration from the high RPM, the connection between the turbine and the DC generator is balanced. Dampening dissipates vibration caused by the rotating high-velocity air. Piping meeting the specifications of the temperature and pressure routed the compressed air from the tank to the air motor. We used a ½ inch quick-connect fitted tubing to connect these various components. We aimed to construct a completely modular design. This goal required our team to design and build a mounting system for the drill and motor. This housing allows a user to transport the system to different environments where its application is needed. The tank, due to its size, will remain a separate component of the design [21, 22].

Table 3: Selected components for the small-scale CAES build.

Item	**Image**	**Cost**	**Specifications**
Air Tank: *Husky 20 Gal. 2Oil-FreeOil Free Portable Vertical Electric Air Compressor*	 Air Tank	$299.00	- 20 gal - 200 psig - 1.3 HP - 4 CFM @ 90 psig
Drill: *Husky 3/8 in. Keyed Chuck Reversible Drill*	 Drill	$54.98	- 2000 RPM at 90 psig - Reversible
Motor: *Granger DC Permanent Magnet Motor, 1/35 HP*	 Motor	$48.05	- 12 V - DC motor - 1/35 HP

3.3 Thermodynamic Analysis

Next, we performed preliminary thermodynamic analyses to understand the theoretical temperatures and pressures at various stages in the basic CAES system. The basic CAES system is detailed above in Figure 1, with the compressor and tank working from the manufacturer and no changes to the system. First, we performed a thermodynamic analysis on the compressor.

The following analyses solve the various temperatures and pressures before and after compression. Figure 5 below depicts the input at stage 1, before compression, and the output of the compressor at stage 2. All calculations assume that the input pressure (P_1) and input temperature (T_1) are standard values, 101 kPa and 293K, respectively. Table 4 details all input values used in the thermodynamic analysis. We detail two compressor analyses: isentropic compression and isothermal compression. Table 5 details the Husky storage tank and compressor specifications, provided directly from the manufacturer.

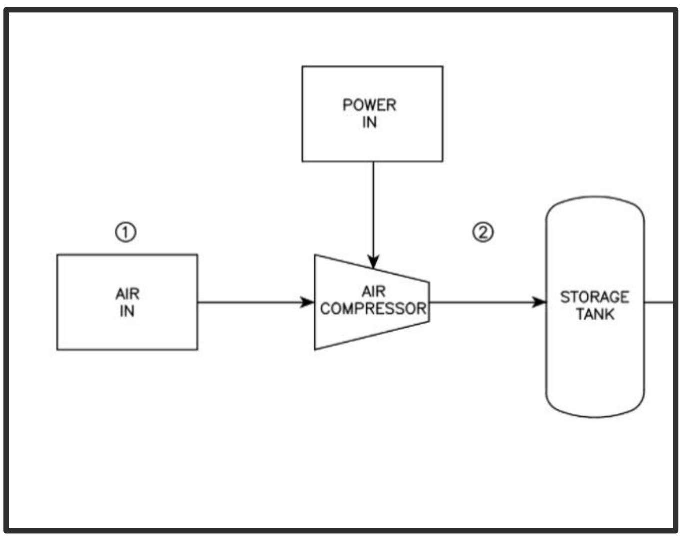

Figure 5: Compressor and Storage Tank Stages

Table 4: Inputs Used in Thermodynamic Analyses

Constant	Value	Units
Input Temperature (T_1)	293	K
Input Pressure (P_1)	101	kPa
Enthalpy In (h_1)	293.15	kJ/kg K
Universal gas constant (R)	0.287	kJ/kg K
Ratio of specific heats	1.4	-
Max Tank Pressure (P_2)	1480	kPa

Table 5: Air Compressor and Tank Specifications from Manufacturer

Tank Specification	Value	Units
Maximum pressure in tank	1379	kPag (gauge pressure)
	1480	kPa
Maximum pressure outlet of tank	620	kPag (gauge pressure)
	721	kPa
Tank Volume (V)	20	gal
	0.0757	m^3
Tank Height (excluding wheel and compressor heights)	30	in
	0.762	m
Tank Width	17	in
	0.4318	m
Tank Depth	17	in
	0.4318	m
Mass flow rate in	0.002	kg/sec
Air Delivery (at 90 psi)	4	SCFM
Air Delivery (at 40 psi)	5.2	SCFM
Product Weight	67	lbs.
Horsepower	1.3	hp

3.3.1 Isentropic Compression Analysis

Isentropic compression is where the entropy of the system remains constant. The following analysis solved for the ideal maximum temperature of the air after compression, without any losses. This is an ideal temperature, that provides us with a maximum *ideal* value. While we understood the air in the rank would not reach this isentropic maximum temperature, this analysis provided a maximum value or frame of reference for further design planning.

Assumptions:

- No heat loss during compression
- No cooling during compression
- Standard atmospheric pressure and temperature (T_1= 293 K and P_1= 101 kPa)
- Compressor pressure ratio (PR)= 1480 kPa/101 kPa= 14.6
- Compressor efficiency = 0.8 = 80%

Isentropic Compression Equation:

$$\frac{T_{2s}}{T_1} = \left(\frac{P_2}{P_1}\right)^{\frac{k-1}{k}} \tag{2}$$

Where:

T_{2s} = isentropic outlet temperature [K]

T_1 = inlet temperature [K]

P_1 = inlet pressure [kPa]

P_2 = outlet pressure [kPa]

k =specific heat ratio

Rearrange Equation 2 to solve for T_{2s}:

$$T_{2s} = T_1 \left(\frac{P_2}{P_1}\right)^{\frac{k-1}{k}}$$

Plug in values to solve for T_{2s}:

$$T_{2s} = 293\ K \left(\frac{1480\ kPa}{101\ kPa}\right)^{\frac{1.4-1}{1.4}}$$

T_{2s} result:

$$\boldsymbol{T_{2s} = 630.95\ K}$$

$$\boldsymbol{h_{2s} = 638.63\ kJ/kg}$$

630.95 K is the *ideal* maximum temperature the air filling the storage tank will reach. We determined the isentropic enthalpy at stage 2, h_{2s}, from the thermodynamic table; we used a temperature of 630 K as an approximation.

Compressor Efficiency Equation:

$$\eta_{comp} = \frac{h_{2s} - h_1}{h_2 - h_1} \times 100 \tag{3}$$

Where:

η_{comp}= compressor efficiency [%]

T_{2s}= isentropic outlet temperature [K]

T_1= inlet temperature [K]

T_2= actual outlet temperature [K]

Rearrange Equation 3 to solve for h_2:

$$h_2 = \frac{h_{2s} - h_1}{\eta_{comp}/100} + h_1$$

Solve for the *actual* enthalpy using an assumed compressor efficiency of 0.8 or 80%:

$$\mathrm{h_2} = \frac{630.95\ \mathrm{kJ/kg} - 293.15\ \mathrm{kJ/kg}}{0.8} + 293.15\ \mathrm{kJ/kg}$$

h_2 result:

$$\boldsymbol{h_2 = 715.40\ kJ/kg}$$

Using the thermodynamic table, estimate T_2 using h_2

$$\boldsymbol{T_2 = \sim 700\ K}$$

700 K is the actual maximum temperature the air can reach, given the assumption there are no heat losses in the tank. However, this is a completely idealized analysis. Through testing and

design validation, we never measured a temperature even close to this due to the difference between tank equilibrium and compressor equilibrium.

Most commercial small air compressors, used without oil, are maintained to typical outlet air temperatures of 160-180 °C, or about 433-453 K [24]. The theoretical maximum temperature from our analysis of about 700 K, under the assumption of no heat loss or cooling of the compressor, is quite high. The difference between our calculated theoretical temperature and the typical temperature, provided by small compressor manufacturers, is about a 250 K difference. However, it is known that our Husky compressor utilizes compressor cooling. Outside air is used to compress the air and compressor elements. This theoretical calculation under the assumption of no heat loss or compressor cooling helps to identify the importance of compressor cooling in the system. Table 6 details the isentropic compression results for stage 2 of the system.

Table 6: Isentropic Compression Analysis Stage 2 Results

Variable	**Value**	**Units**
T_{2s}	630.95	K
T_2	700	K
P_2	1480	kPa
h_2	715.40	kJ/kg

Next, we determined the work of the compressor.

Work of Compressor:

$$W_C = (h_2 - h_1) \tag{4}$$

Where:

W_C = work of the compressor [kJ/kg]

h_2 = stage 2 enthalpy [kJ/kg]

h_1 = inlet, stage 1, enthalpy [kJ/kg]

Plug in values:

$$W_C = (715.40\ kJ/kg) - (293.15\ kJ/kg)$$

W_C result:

$$\boldsymbol{W_C = 422.25\ \mathrm{kJ/kg}}$$

3.3.2 Isentropic Expansion Analysis

Next, we calculated the theoretical values for the temperatures leaving the tank and turbine. Figure 6 below details stages 3 and 4 used in the analysis. Stage 3 is leaving the tank, where the pressure is regulated, and stage 4 after the air is expanded through the turbine.

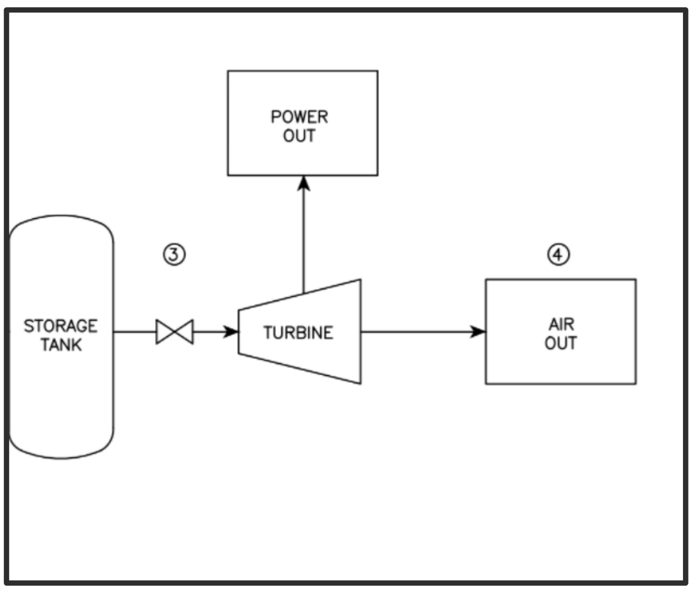

Figure 6: Storage tank and turbine stages

Assumptions:

- Air expands to atmospheric conditions (P_4 = 101 kPa)
    - Pressure ratio of turbine = 721 kPa/101 kPa = 7.1

The Husky air storage tank contains a regulator valve that controls the exit pressure of the air leaving the tank. The maximum pressure of the air leaving the tank is 721 kPa. Table 10 below details the stage 3 values after the air is regulated from 1480 kPa to 721 kPa.

Table 7: Tank Valve Outputs

Variable	Value	Units
T_2	700	K
P_2	1480	kPa
h_2	715.40	kJ/kg
T_3	700	K
P_3	721	kPa
h_3	715.40	kJ/kg

Next, we determined the pressure, temperature, and enthalpy at the exit of the system. The following isentropic analysis determines the output values at the exit, stage 4.

Isentropic Expansion Equation:

$$\frac{T_{4s}}{T_3} = \left(\frac{P_4}{P_3}\right)^{(k-1)/k} \tag{5}$$

Rearrange Equation 5 to solve for T_{4s}:

$$T_{4s} = T_3 \left(\frac{P_4}{P_3}\right)^{(k-1)/k}$$

Plug in values to solve for T_{4s}:

$$T_{4s} = (700\ K)\left(\frac{101\ KPa}{721\ KPa}\right)^{(1.4-1)/1.4}$$

T_{4s} result:

$$\boldsymbol{T_{4s} = 399.21\ K}$$

Estimate h_{4s} using thermo table (estimated from 400 K):

$$\boldsymbol{h_{4s} = 400.98\ K}$$

Turbine Efficiency Equation:

$$\eta_{turbine} = \frac{h_3 - h_4}{h_3 - h_{4s}} \times 100 \tag{6}$$

Rearrange Equation 6 to solve for h_4:

$$h_4 = h_3 - [\eta_{turbine}(h_3 - h_{4s})]$$

Plug in values to solve:

$$h_4 = 715.40 - [0.90(715.40 - 399.21)]$$

h_4 result:

$$\boldsymbol{h_4 = 430.83\ kJ/kg}$$

Estimate T_4 using thermo table:

$$\boldsymbol{T_4 = {\sim}430\ K}$$

After we determined the stage 4 temperatures and enthalpies, we calculated the work of the turbine.

Work of the turbine:

$$W_T = h_3 - h_4 \tag{7}$$

Where:

W_T = work of the compressor [kJ/kg]

h_4 = stage 4 enthalpy [kJ/kg]

h_3 = stage 3 enthalpy [kJ/kg]

Plug in values:

$$W_T = (715.40\ kJ/kg) - (430.83\ kJ/kg)$$

Work of the turbine result:

$$\boldsymbol{W_T = 284.57\ kJ/kg}$$

Overall Efficiency of the System:

$$\eta_{overall} = \frac{W_C - W_T}{W_C} \times 100 \tag{8}$$

Plug in W_C and W_T and solve:

$$\eta_{overall} = \frac{422.25 \ - \ 284.57}{422.25} \times 100$$

Overall system efficiency result:

$$\boldsymbol{\eta_{overall} = 32.61}\ \%$$

The complete isentropic analysis of the basic CAES system, under the assumption of no heat loss, found an overall system of 32.61%.

Table 8: Isentropic Analysis Results Summary

Variable	**Value**	**Units**
T_{2s}	630.95	K
T_2	700	K
P_2	1379	KPa
h_{2s}	638.63	kJ/kg
h_2	715.40	kJ/kg
T_3	691.0	K
P_3	721	kPa
h_3	715.40	kJ/kg
T_{4s}	399.21	K
T_4	430	K
P_4	101	kPa
h_{4s}	400.98	kJ/kg
h_4	440.65	kJ/kg

3.3.3 Isothermal Compression Analysis

The next compression analysis assumes isothermal compression. Isothermal compression assumes the compressor cools completely and the temperature remains constant during compression.

Assumptions:

- No change in enthalpy
  - $T_1 = 293K = T_2 = 293K$

Work Integral Equation:

$$\dot{W} = \dot{m}_{in} \int_{V_i}^{V_f} \frac{RT}{P} Dp \quad (9)$$

`

Where:

$\dot{W}$ = work [kJ/s]

$\dot{m}_{in}$ = mass flow rate into the compressor [kg/sec]

R = universal gas constant= 0.287 [kJ/kg K]

T = temperature [K]

V_i = initial volume [m^3]

V_{f} = final volume [m^3]

Integrate Equation 9:

$$\dot{W} = \dot{m}_{in} RT ln\left(\frac{P_2}{P_1}\right) \quad (10)$$

Plug in knowns to Equation 10 to solve for $\dot{W}$:

$$\dot{W} = (0.0019\ kg/s)(0.287\ kJ/kgK)(293K)\ln\left(\frac{1480\ KPa}{101\ KPa}\right)$$

$\dot{W}$ result:

$$\boldsymbol{\dot{W} = 0.428\ kJ/s\ =\ 0.428\ kW}$$

0.428 kW equals the power needed to run the compressor if the air is completely cooled during compression.

3.4 Storage Tank Theoretical Analyses

The filling and emptying of the air tank are both dependent on time. The maximum tank pressure of 1379 kPag (200 psig) is not reached instantly as the tank fills with air overtime during compression. Similarly, the tank can also provide an output of air as it empties for a specific amount of time. The following analyses examine the changing pressures and temperatures of air in the storage tank. Two separate analyses are completed: one for the tank filling stage and one for the tank emptying stage.

3.4.1 Tank Filling

As time increases, the temperature and pressure of the air in the storage tank also increases. The following analysis solves the changing temperatures and pressures as a function of time.

Assumptions:

- No heat loss through the tank
- h_{in} = constant
- Use average values for c_p and c_v based on the starting pressure and temperature of our system
  - c_p= specific heat at constant pressure = 1.005 kJ/kg K
  - c_v= specific heat at constant volume = 0.7525 kJ/kg K
- Constant mass flow rate while filling the tank (constant $\dot{m}_{in}$)
- gamma= specific heat ratio= c_p/c_v = 1.4

Mass Flow Rate Equation:

$$\dot{m} = \frac{dm}{dt} \tag{11}$$

Where:

$\dot{m}$= mass flow rate [kg/sec]

dm= change in mass [kg]

dt= change in time [seconds]

Integrate Equation 11 to solve mass as a function of time for tank filling:

$$m(t) = m_0 + (\dot{m}_{in} t) \tag{12}$$

Where:

m_o = initial mass of air in tank based on STP [kg]

$\dot{m}_{in}$ = mass flow rate [kg/sec]

t = time (seconds)

m(t) = mass of air at any given time *t* [kg]

Ideal Gas Law Equation:

$$PV = mRT \tag{13}$$

Where:

P=pressure [psi]

V=volume [m^3]

m=mass [kg]

R=gas constant=0.287 [kJ/kg K]

T=temperature [K]

Combine Equations 12 and 13:

$$\dot{m} h_{in} = \frac{d(mc_v T)}{dt}$$

Expand equation:

$$\dot{m} h_{in} t = (mc_v T) - (m_i c_v T_i)$$

Rearrange to solve for temperature as a function of time:

$$T(t) = \frac{(\dot{m} h_{in} t) + (m_i c_{vi} T_i)}{(m_o + \dot{m} t) c_{vf}} \tag{14}$$

Where:

T(t) = temperature at any given time t [K]

$\dot{m}$ = mass flow rate in [kg/s]

h_{in} = enthalpy in [kJ/kg]

m_o = initial mass of air in the tank [kg]

c_{vi} = initial specific heat of air in constant volume (based on a T= 293K)

T_i = initial temperature in the tank [K]

t = time [seconds]

c_{vf} = final specific heat of air in a constant volume (use an average c_v based on minimum and maximum temperatures)

Rearrange Equation 13 to solve for pressure:

$$P = \frac{mRT}{V} = \frac{mRT(t)}{V} \tag{15}$$

Plug Equation 14 into Equation 15 to solve pressure as a function of time:

$$P(t) = \frac{(m_o + \dot{m}t)RT(t)}{V} \tag{16}$$

Equations 14 and 16 require the initial mass of air in the tank. We calculated the initial mass of air in the tank (before compression) using the ideal gas equation, presented in Equation 13.

Rearrange Equation 13 to solve for mass:

$$m = \frac{PV}{RT}$$

Plug in known values into Equation 12 to solve for initial mass of air in the tank (assuming STP):

$$m_o = \frac{(101.35\ KPa)\ (0.0757\ m^3)}{(0.287\ kJ/kgK)(293\ K)}$$

m_o result:

$$\boldsymbol{m_o = 0.0912\ kg}$$

The initial mass of the air in the tank (assuming STP) is 0.0912 kg. Next, the tank filling equations T(t) and P(t) were plotted using the inputs in Table 9. This preliminary analysis was based on the maximum isentropic temperature calculated above, 691 K. Temperature vs. time and pressure vs. time plots were generated for the tank filling, presented below.

Table 9: Constants for Tank Filling Analysis

Constant	**Value**	**Units**
R_{air}	0.287	kJ/kg K
Mass flow rate in ($\dot{m}$)	0.002	kg/s
Enthalpy in (h_{in})	425	kJ/kg
c_p	1.005	kJ/kg K
Initial Mass in tank(m_o)	0.0912	kg
Initial temperature (T_1)	293	K
Volume (V)	0.0757	m^3
c_{vi}	0.7172	kJ/kg K
*c_{vf}	0.75245	kJ/kg K

**Based on an average c_v, evaluated based on the specific heat of air @ 293 K and 101 KPa (0.7172 kJ/kg K) and the specific heat of air @ 691K and 1379 KPa (0.75245 kJ/kg K).*

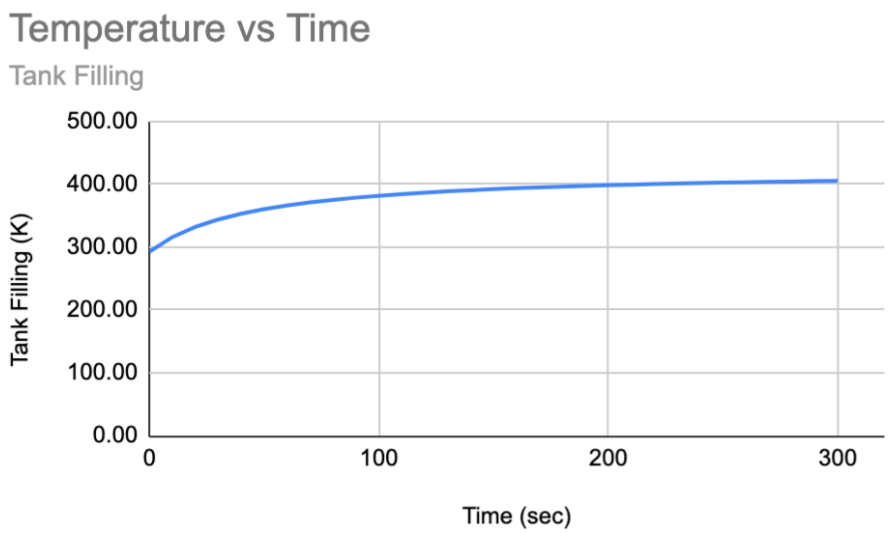

Figure 7: Theoretical temperature vs. time plot for tank filling

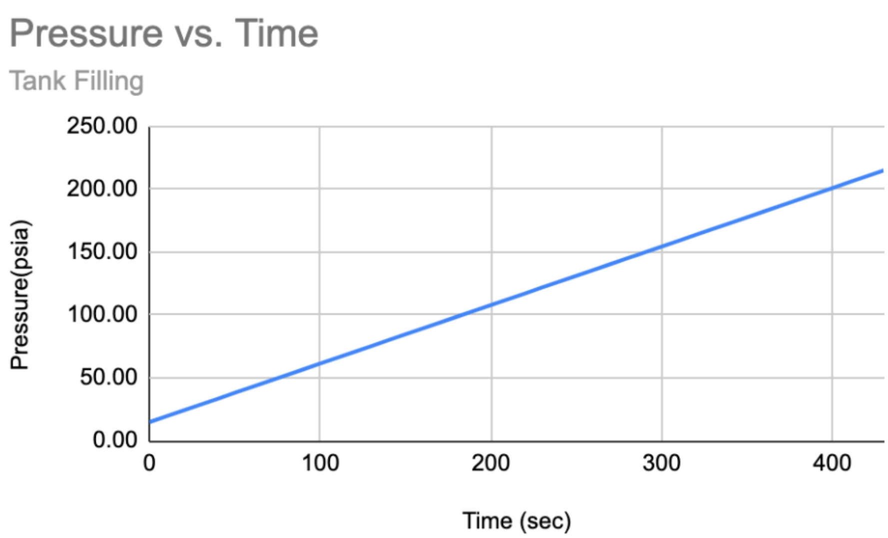

Figure 8: Theoretical pressure vs. time plot for tank filling.

Table 10: Theoretical Tank Filling Results

Variable	Value	Units
Time to fill	~430	seconds
	~7.17	minutes
Mass of air in tank when filled (to 200 psig)	0.95	kg
Temperature of air when filled (to 200 psig)	410.25	K
Pressure of air when filled (to 200 psig)	214.91	psia

Our preliminary analysis determined an approximate time to fill the tank of about 430 seconds, or about 7.17 minutes. The theoretical mass of air in the tank when full is about 0.95 kg.

3.4.2 Tank Emptying

The tank emptying analysis is similar to the tank filling analysis above. However, as time increases and the tank is emptied, the temperature and pressure of the air decrease over time. The following analysis solves the changing temperatures and pressures as a function of time.

Assumptions:

- Changing mass flow rate as a function of time ($\dot{m}(t)$) based on changing temperature and pressure in the tank
- Assume a Mach=1 (choked flow) for flow exiting the tank
  - Choked Flow (exiting the storage tank)
  - Velocity is choked when the Mach=1
  - Subsonic flow when Mach<1
  - Supersonic flow when Mach>=1
- c_p and c_v used are average values based on an average value between the minimum temperature of 293 K and maximum temperature reached 420 K
  - Average c_p= 1.005 kJ/kg K
  - Average c_v=0.7525 kJ/kg K
- Constant exit area in the tube - no decrease in tube dimension

Mass of air in the tank at any given time t (while emptying):

$$m_f(t) = m_i - (\dot{m}_{out} t) \tag{17}$$

Where:

m_o = initial mass of air in tank based on STP [kg]

$\dot{m}_{out}$ = mass flow rate [kg/sec]

t = time [seconds]

m(t) = mass of air at any given time *t* [kg]

Combine Equations 13 and 17:

$$\dot{m}_{out} c_p T_f = -\frac{d(m c_v T_f)}{dt}$$

Expand equation:

$$\dot{m}_{out} c_p T_f = \frac{(m_i c_v T_i) - (m_f(t) c_v T_f(t))}{\Delta t}$$

Rearrange to solve for temperature as a function of time:

$$T_f(t) = \frac{m_i c_v T_i}{(\dot{m}_{out} \Delta t c_p) + (m_i - (\dot{m}_{out} t)\ c_v)} \tag{18}$$

Where:

T(t)= temperature at any given time [K]

T_i= initial temperature when tank is full [kg]

m_i= mass of air in tank when tank is full [kg]

Using the ideal gas law, the T(t) is used to solve pressure as a function of time:

$$P = \frac{mRT}{V} = \left[\frac{mR}{V}\right]\left[T_f(t)\right]$$

Plug in Equation 18 into the ideal gas law above:

$$P_f(t) = \left[\frac{m_i c_v T_i}{(\dot{m}_{out} \Delta t c_p) + (m_i - (\dot{m}_{out} t)\ c_v)}\right]\left[\frac{mR}{V}\right] \quad (19)$$

Choked Flow Equation (Uses the assumption of a Mach=1):

$$\dot{m} = \frac{Ap_t}{\sqrt{T_t}}\sqrt{\frac{\gamma}{R_{air}}}\left(\frac{\gamma+1}{2}\right)^{-\frac{\gamma+1}{2(\gamma-1)}} \quad (20)$$

Where:

$\dot{m}$ = mass flow rate [kg/s]

A = Exit area [m^2]

p_t = total pressure [KPa]

T_t = total temperature [K]

R_{air} = 0.287 [kJ/kg K]

γ = gamma = 1.40

Reduce the right side of Equation 20 to a constant called "choked flow constant':

$$choked\ flow\ constant = \sqrt{\frac{\gamma}{R_{air}}}\left(\frac{\gamma+1}{2}\right)^{-\frac{\gamma+1}{2(\gamma-1)}} \quad (21)$$

Plug in values:

$$choked\ flow\ constant = \sqrt{\frac{1.40}{0.287\ kJ/kg\ K}}\left(\frac{1.40+1}{2}\right)^{-\frac{1.40+1}{2(1.40-1)}}$$

Choked flow constant value:

$$choked\ flow\ constant = 1.278$$

Equation 20 simplifies:

$$\dot{m} = \frac{Ap_t}{\sqrt{T_t}}(choked\ flow\ constant) \quad (22)$$

We solved the tank emptying analysis in 10-second iterations. For each iteration, we used the previous mass flow rate to solve the new pressure and temperatures at the time, as the mass flow rate is a function of pressure and temperature as well, changing with time. For example, at 20 seconds, we use mass flow rate from the 10-second interval to solve for P and T at the 20-second interval. Then, we found a new mass flow rate value for the 20-second interval.

Table 11: Constants for Tank Emptying Analysis

Constants	Value	Units
c_p	1.008	kJ/kg K
Gamma	1.40	
R_{air}	0.287	kJ/kg K
Choked flow constant	1.278	-
Area	0.0000316531	m^2
Mass in tank	0.93	kg
Initial temperature	410	K

Temperature vs. time and pressure vs. time plots were generated for the tank filling.

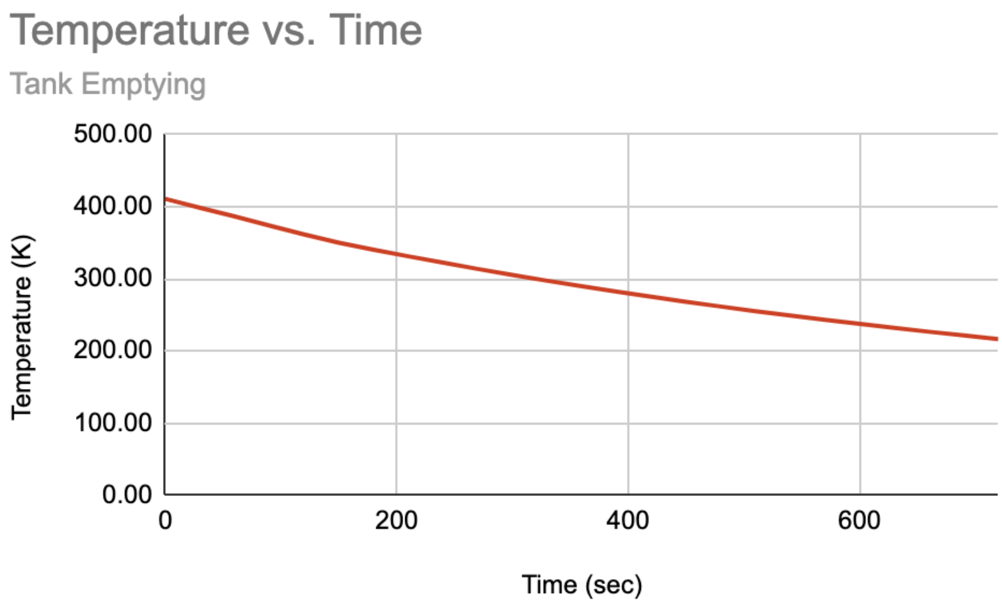

Figure 9: Theoretical temperature vs. time plot for tank emptying.

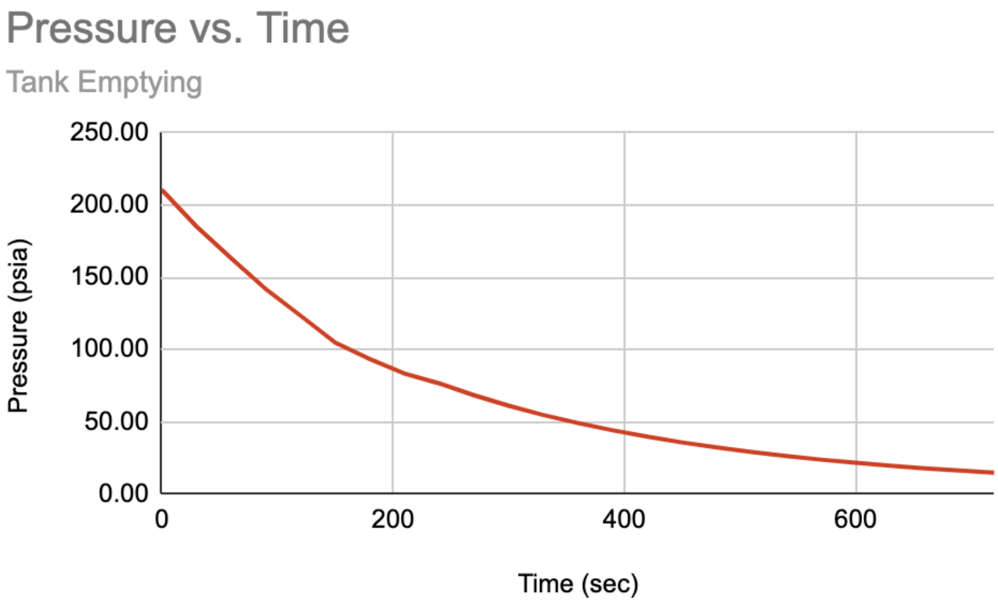

Figure 10: Theoretical pressure vs. time plot for tank emptying.

Table 12: Theoretical Tank Emptying Results

Variable	Value	Units
Time to empty	~720	seconds
	12	minutes
Mass of air in tank when emptied	0.12	kg
Temperature of air when emptied	216.44	K
Pressure of air when emptied	101	KPa

3.5 Heat Loss and Insulation Analyses

Next, we conducted a heat loss analysis to determine the total heat loss between the compressed air and the storage tank. To solve the total heat loss between the compressed air and the storage tank, we used thermal resistance circuits as a heat loss problem solving strategy.

Constant	Value	Units
Maximum theoretical temperature of air (T_{max})	410	K

Radius of tank to the outside wall (r_1)	0.2195	m
Radius of tank to the inside wall (r_2)	0.2132	m
Height of tank (h)	30	in
	0.7620	m
Free convective heat transfer coefficient of air (h_{air})	4	$W/m^2 K$
Thermal conductivity of steel (k_{steel})	45	W/m K
Thickness of the tank wall (L)	0.0063	m
Surface area of the outside of tank (A)	1.35	m^2

Table 13: Constants for Heat Loss Analysis

3.5.1 Thermal Resistance

Assumptions:

- Average thickness of steel air storage tanks (since we cannot accurately measure the tank thickness)
- Average conductivity of steel (45 W/m K)
- Treat tank as a cylindrical wall
    - Estimate surface area of tank using a surface area of cylinder approximation
- Laminar flow

The resistance calculation assumes of three resistances: the air inside the tank, the steel tank, and the air outside the tank. Figure 13 below depicts the resistance setup.

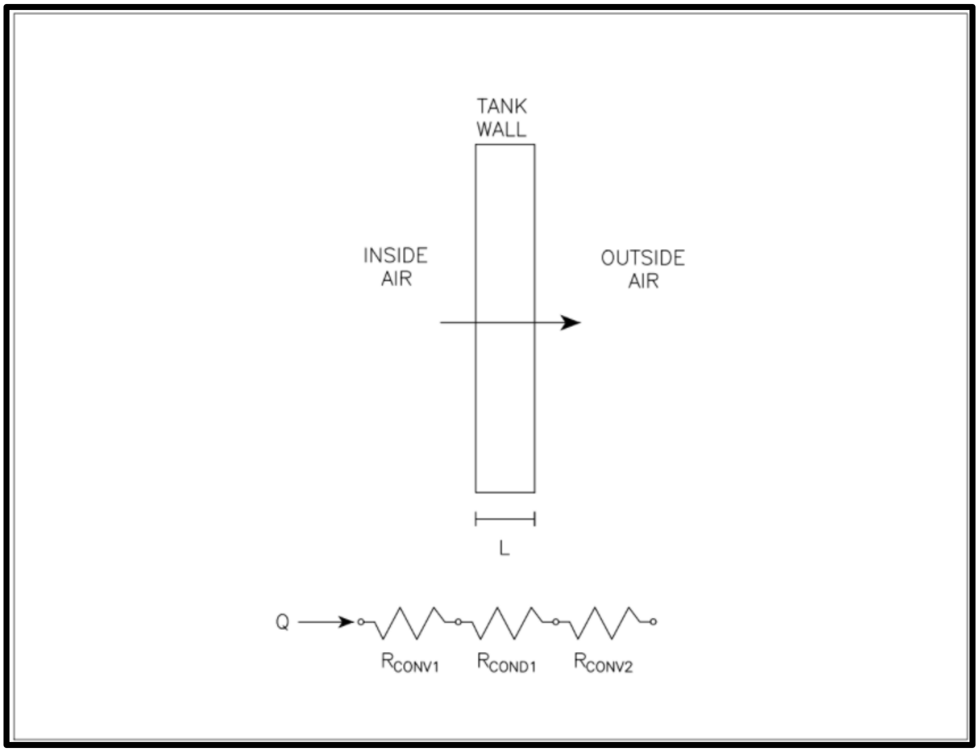

Figure 11: Thermal resistance diagram without insulation.

Convection Thermal Resistance Equation for Plane Wall:

$$R_{conv} = \frac{1}{h\,\mathrm{A}} \tag{23}$$

Where:

R_{conv} = convective thermal resistance [K/W]

h_{air} = Convective heat transfer coefficient of air [W/m^2 K]

A = Surface area of the outside of tank [m^2]

Conduction Thermal Resistance Equation for Cylindrical Wall:

$$R_{cond} = \frac{ln(r_1 \,/\, r_2)}{2\pi Lk} \tag{24}$$

Where:

R_{cond} = conductive thermal resistance [K/W]

k_{steel} = Thermal conductivity of steel [W/m K]

L = Thickness of the tank wall [m]

r_1 = Radius of tank to the outside wall [m]

r_2 = Radius of tank to the inside wall [m]

Combine Equations 23 and 24 to solve the total thermal resistance of storage tank equation:

$$R_{eq} = \frac{1}{h_{air}A} + \frac{ln(r_1 / r_2)}{2\pi L k_{steel}} + \frac{1}{h_{air}\mathrm{A}} \tag{25}$$

Where:

R_{eq}= total thermal resistance [K/W]

Equation 23 above requires the heat transfer coefficient of air. While there are approximations, Equation 25 is a more accurate estimate of this variable, as Equation 25 accounts for the tank height and temperature difference.

Heat transfer coefficient of air (vertical plane or cylinder/laminar flow) equation:

$$h_{air} = 1.42\left(\frac{\Delta T}{L}\right)^{1/4} \tag{26}$$

Where:

h_{air} = heat transfer coefficient of air [W/m^2 K]

ΔT = change in temperature [K]

L =height of vertical wall [m]

Plug in knowns to Equation 26:

$$h_{air} = 1.42\left(\frac{410\ - 293\ K}{0.7620\ m}\right)^{1/4}$$

Heat transfer coefficient of air result:

$$\boldsymbol{h_{air}} = \mathbf{5.00\ W/m^2\ K}$$

Equation 25 requires the surface area of the storage tank. We calculated the surface area using Equation 27, the surface area of a cylinder.

Surface Area of a Cylinder Equation:

$$Surface\ Area = 2\pi rh + 2\pi r^2 \tag{27}$$

Where:

r = radius of tank [m]

h= height of tank [m]

Plug in and solve:

$$Surface\ Area = 2\pi(0.2195\ m)(0.7620\ m) + 2\pi(0.2195\ m)^2$$

Outside surface area of the tank result:

$$\boldsymbol{Surface\ Area = 1.35\ m^2}$$

Plug in all known values into Equation 17:

$$R_{eq} = \frac{1}{(5\ W/m^2K)(1.35\ m^2)} + \frac{ln(\ 0.2195m/0.2132m)}{2(\pi)(0.0063m)(45\ W/mK)} + \frac{1}{(5\ W/m^2K)(1.35\ m^2)}$$

Total resistance result:

$$\boldsymbol{R_{eq} = 0.31\ K/W}$$

The resistance of the air dominates over steel. The resistance of the air is 0.148 K/W. The resistance of the air term appears twice in the overall resistance equation, as there is air inside of the tank, as well as outside of the tank. The resistance of the steel is only about 0.0163 K/W; this is about 9 times smaller than the resistance of air alone.

3.5.2 Insulation

Next, we calculated the total heat loss in the tank.

Heat Loss Equation:

$$q = \frac{\Delta T}{R_{eq}} \tag{28}$$

Where:

q = heat loss [W]

R_{eq} = Total thermal resistance [K/W]

ΔT = Difference between starting and ending temperatures [K]

Using the temperatures solved during the preliminary thermodynamic analysis calculations, we solved the potential heat loss at the tank under both scenarios.

Plug in values and solve:

$$q = \frac{(410.0K - 293.00K)}{0.31\ K/W}$$

Result:

$$\boldsymbol{q = 377.42\ W = 0.377\ kW}$$

$$\boldsymbol{q = 377.42\ J/sec}$$

This analysis provided our team with perspective on how much energy is lost with the tank walls. Following this analysis, we estimated there are about 377 Joules of energy lost per second.

The next set of calculations solves for the amount of insulation needed to decrease the amount of heat loss. These calculations are based on the assumption of only 100 W of heat loss. R-value for insulation depends on the type of insulation, thickness, and density. The higher the R-value, the higher insulation there is. The U.S. Department of Energy recommends the installation of a water heater blanket with the R-value of 1.41m^2 K/Wd [26]. Figure 14 below shows the thermal resistance diagram of this setup.

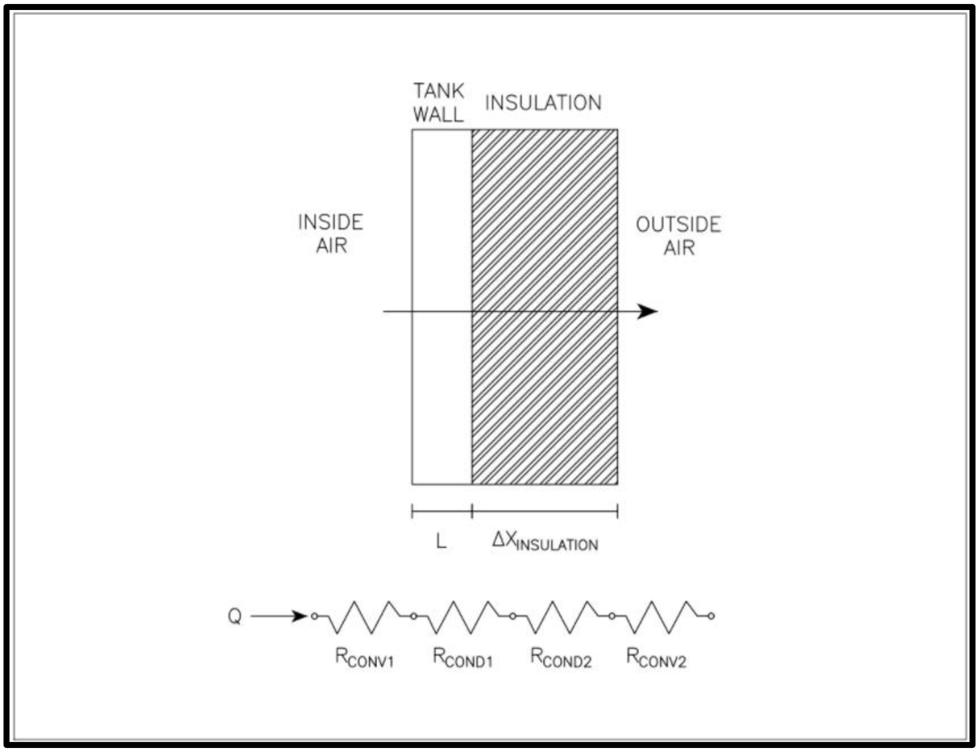

Figure 12: Thermal resistance diagram with insulation

Using the same analysis procedure above, we completed another iteration of calculations. However, instead of solving the heat loss, Q, we instead picked an appropriate value of heat loss and solved backward for the thickness of insulation required. We performed this set of calculations using an assumed heat loss of 100 W. This analysis assisted our team in later selecting an appropriate type of insulation.

Assumptions:

- $q_{insulated}$ = 100 W
- Insulation type: fiberglass insulation
  - Fiberglass insulation thermal conductivity= 0.04 W/m K [27]

Rearrange equation 28 to solve for $R_{eq(insulated)}$:

$$R_{eq(insulated)} = \frac{\Delta T}{q_{insulated}}$$

Plug in values and solve:

$$R_{eq(insulated)} = \frac{(410.0K - 293.00K)}{100 \text{ W}}$$

$R_{eq(insulated)}$ result:

$$R_{eq(insulated)} = 1.17 \text{ K/W}$$

Insulation Resistance Equation:

$$R_{insulation} = \frac{\Delta x_{insulation}}{kA} \tag{29}$$

Where:

$R_{insulation}$ = insulation resistance [K/W]

$\Delta x_{insulation}$ = thickness of insulation (m)

k =thermal conductivity of insulation [W/m K]

A = surface area of tank [m^2]

Combine Equations 22 and 25 to solve for a new equivalent total resistance:

$$R_{eq(insulated)} = R_{conv} + R_{cond} + R_{insulation} + R_{conv} \tag{30}$$

Where:

$R_{eq(insulated)}$ = Equivalent resistance with insulation [K/W]

Simplify Equation 30:

$$R_{eq(insulated)} = R_{eq} + R_{insulation} \tag{31}$$

Rearrange Equation 31 to solve for $R_{insulation}$:

$$R_{insulation} = R_{eq(insulated)} - R_{eq}$$

Plug in known values to solve for $R_{insulation}$:

$$R_{insulation} = (1.17\ K/W) - (0.31\ K/W)$$

$R_{insulation}$ result:

$$R_{insulation} = 0.86\ K/W$$

This value means that insulation we choose must have an R-value of 0.86 K/W to have 100 W of heat loss. Now that the R-value was found, we next calculated the thickness of the insulation required. This step in the analysis is based off of the selection of fiberglass insulation.

Rearrange Equation 26 to solve for $\Delta x_{insulation}$:

$$\Delta x_{insulation} = kAR_{insulation}$$

Plug in values using the chosen fiberglass insulation:

$$\Delta x_{insulation} = (0.04\ \mathrm{W/m\ K})(1.35\ m^2)(0.86\ K/W)$$

$\Delta x_{insulation}$ result:

$$\Delta x_{insulation} = 0.046\ m$$

$$\Delta x_{insulation} = 4.6\ cm$$

Below is a plot of the theoretical heat loss as a function of the thickness of insulation, based on the calculations listed above. The maximum amount of heat we see in our tank is 380 W, therefore we see a heat loss of about 380 W with no insulation displayed on this graph.

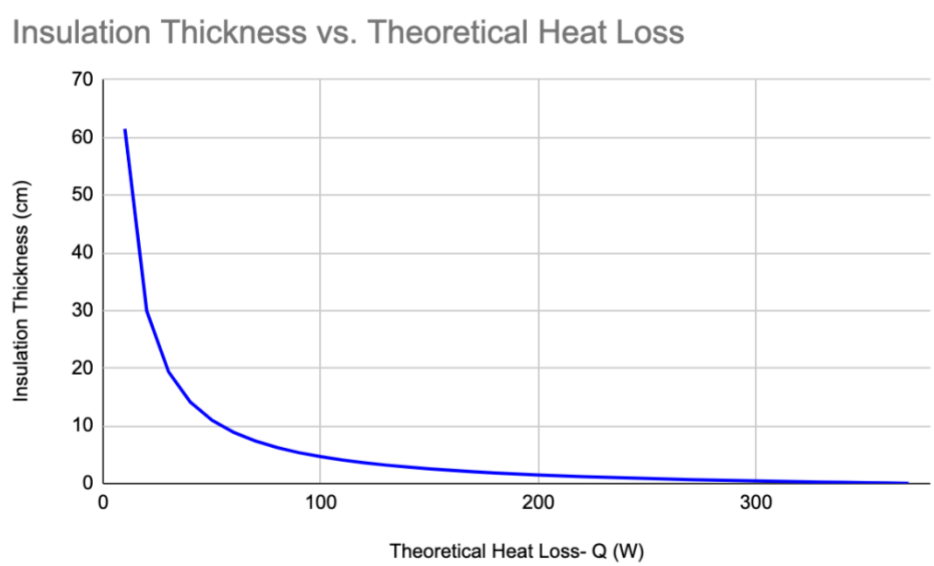

Figure 13: Insulation Thickness vs. Theoretical Heat Loss

Next, we chose a specific type of insulation and calculated the heat loss in the tank with one layer of fiberglass insulation

Assumptions (based on fiberglass insulation):

- Surface area of tank = 1.35 m^2
- Insulation type: fiberglass insulation
    - Fiberglass insulation thermal conductivity= 0.04 W/m K
    - Insulation thickness $= 0.0762\ m$ [27]

Total thermal resistance of storage tank with insulation equation:

$$R_{eq(insulated)} = \frac{1}{h_{air}A} + \frac{ln(r_1 / r_2)}{2\pi L k_{steel}} + \frac{\Delta x_{insulation}}{k_{insulation}A} + \frac{1}{h_{air}\mathrm{A}} \tag{32}$$

Equation 29 simplifies as R_{eq} was solved above:

$$R_{eq(insulated)} = R_{eq} + R_{insulation}$$

$$R_{eq(insulated)} = (0.31\ K/W) + R_{insulation}$$

Thermal resistance of insulation equation:

$$R_{insulation} = \frac{\Delta x_{insulation}}{kA}$$

Plug in known values:

$$R_{insulation} = \frac{(0.0762\ m)}{(0.043\ W/m\ K)\ (1.35\ m^2)}$$

Thermal resistance of insulation result:

$$\boldsymbol{R_{insulation} = 1.31\ K/W}$$

Plug in resistances into Equation 32 to solve the total thermal resistance for the insulated system:

$$R_{eq(insulated)} = (0.31\ K/W) + (1.31\ K/W)$$

Total thermal resistance for the insulated system result:

$$\boldsymbol{R_{eq(insulated)} = 1.62\ K/W}$$

Heat loss with insulation equation:

$$q_{insulated} = \frac{\Delta T}{R_{eq(insulated)}}$$

Plug in known values:

$$q_{insulated} = \frac{(410 - 293\ K)}{(1.62\ \mathrm{K/W})}$$

Heat loss with insulation result:

$$\boldsymbol{q_{insulated} = 72.22\ \mathrm{W}}$$

$$\boldsymbol{q_{insulated} = 72.22\ \mathrm{J/sec}}$$

This new Q value of 72.22 W is our heat loss in the tank. The interpretation of this value is that the tank loses about 72 Joules per second, even when insulated.

Total energy in the tank equation:

$$Q = mc_p\Delta T \tag{33}$$

Where:

Q = heat energy in the tank to start [kJ]

m = mass of air in the tank [kg]

ΔT = change in temperature [K]

Plug in values:

$$Q = (0.95\ kg)(1.005\ kJ/kg\ K)(410 - 293\ K)$$

Total Energy Result:

$$\boldsymbol{Q = 111.71\ kJ}$$

$$\boldsymbol{Q = 111710\ J}$$

3.5.3 Heat Loss Over Time

The heat loss in the tank is also time dependent. We performed two analyses to compare the time it tanks to lose all the heat in the tank, both with and without insulation.

Heat loss in tank time dependence equation:

$$\frac{mc_p dT}{dt} = \frac{(T-293)}{R} \tag{34}$$

Where:

m = mass in tank [kg]

c_p = specific heat capacity of air [kJ/kg K]

dT/dt = change in temperature over change in time

R = resistance [K/W]

T = temperature [K]

Integrate equation 34:

$$\frac{(T-293)}{(410-293)} = e^{(-t/mc_pR)} \tag{35}$$

Using equation 35, we plotted the temperature versus time graphs for both the uninsulated and insulated tanks, using the R values calculated above. Those graphs are shown below.

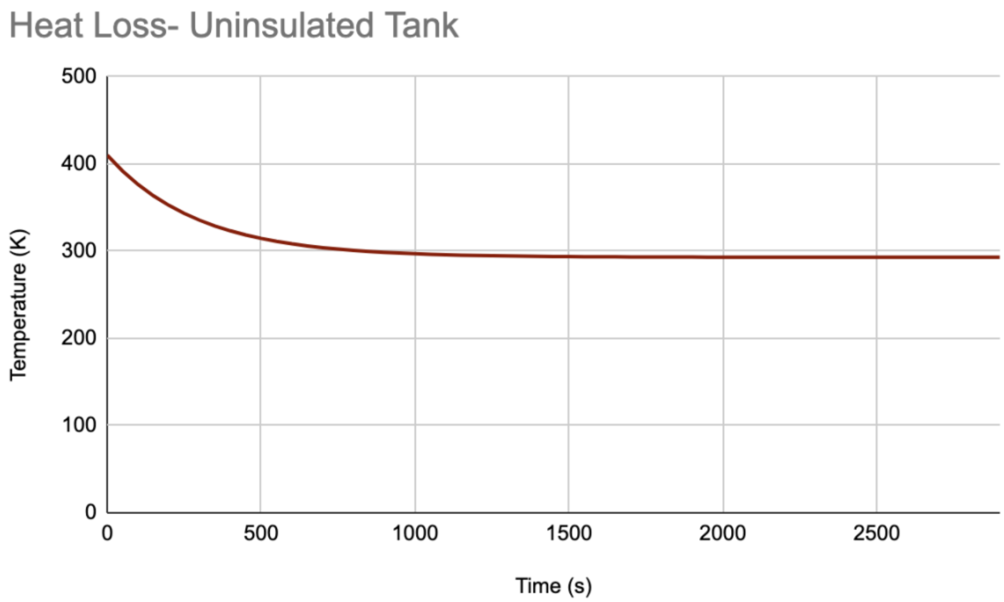

Figure 14: Heat loss in tank over time with no insulation

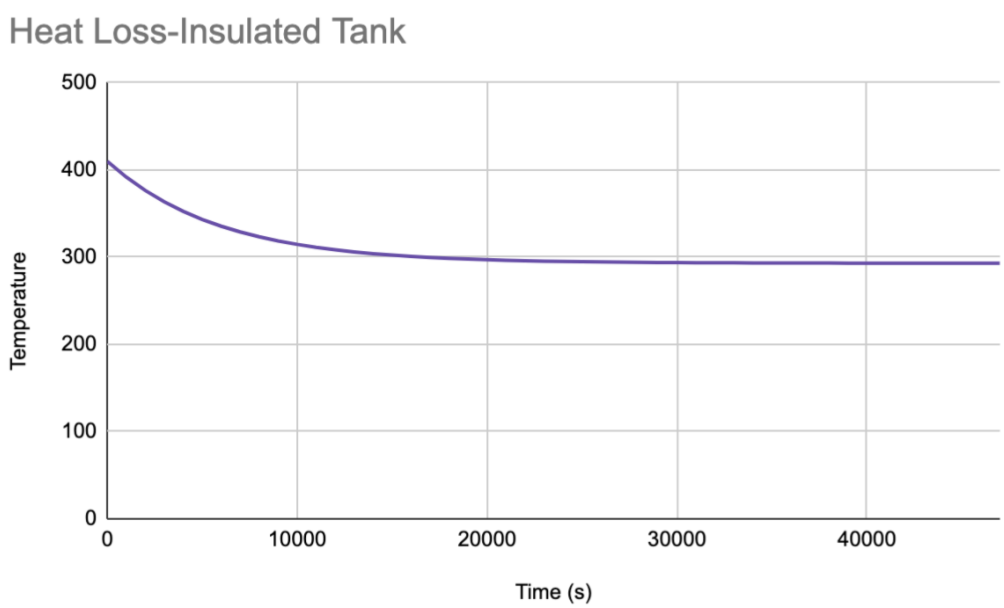

Figure 15: Heat loss in tank over time with insulation

As seen in the figure above, the insulated tank will still lose all of its heat after approximately 30,000 seconds. This translates to 8 1/3 hours, so overnight the insulated tank will lose all of its heat. Due to this, we decided to not pursue this method of testing and instead focused our efforts on the heat exchanger design.

4.0 Methods

This section details the methods used to achieve our goal of improving the efficiency of a CAES system. We first detail how we built drill and motor housing for our system, as well as designed and built the heat exchanger. Lastly, we detail the full set of testing on the heat exchanger system.

4.1 Basic System Testing

After we completed initial thermodynamic and heat loss analyses, we completed initial experimental tests. We ran initial tests on our basic system (i.e., the system without any insulation or cooling system) to verify our initial calculations.

4.1.1 Testing Procedure

Our basic system consists of four main parts. The main piece of the system is the Husky electrical air compressor and 20-gallon tank, that reaches a maximum of 1379 kPag (200 psig). An impact hose connects the air tank to a reversible Husky impact drill. The drill is then connected to a 12 V DC motor.

The basic system testing involved tank emptying and filling. We ran the compressor to fill the air tank to 1379 kPag, and then emptied all the air in the tank. In our preliminary calculations, we used the dimensions and weight of the tank provided by the manufacturer. To validate this weight, we experimentally measured the weight of the tank before and after filling using a scale. We measured the weight of the tank before and after compression for all three trials completed.

While filling the tank, we recorded the total time it took to fill. During filling, we also measured the pressure of the tank and the temperature of compressed air every 30 seconds. To find the temperature of the air, we used a thermocouple attached to a thermal camera and held the end to a predetermined spot on the metal wire connecting the compressor to the tank.

Alongside the tank filling experiments, our team wanted a baseline for how long it would take to empty the tank and the amount of voltage we could generate. The 20-gallon Husky tank regulates the air leaving the tank at 620 kPag (90 psig). We connected the impact hose to the storage tank and let the air out through the drill not attached to the motor (for safety purposes). We measured the voltage during emptying and took a reading every 30 seconds. Since we were unable to accurately measure the temperature of the air within the tank, we only gathered information on the change in pressure over time.

We recognized that realistically, the compressed air would sit in the tank over time before being used more often than immediately being compressed and used to generate electricity. This would allow the compressed air to cool within the tank and would lead to energy losses. To simulate this and predict the amount of thermal energy lost over time, our team measured the rough temperature of the outside of the tank every five minutes over a forty-minute time period. To estimate the tank temperature, we used the thermal camera to take measurements of the temperature at the top and bottom of the tank and averaged the two. Due to time, we also only ran this test once.

4.1.2 Preliminary Results and Analysis

The calculated mass of the tank and air are detailed in Table 9. The mass of the air added to the tank due to compression remained consistent at 1.04 kg. The previously calculated mass flow rate into the tank was smaller than the actual mass flow rate observed due to the longer time to fill observed in the experiment. We determined the mass flow rate into the tank using the expected change in mass divided by the calculated time to fill. The theoretical time to fill was 200 seconds shorter than the experimental time. Comparable changes in mass were observed, resulting in the difference between calculated and experimental mass flow rate into the tank.

Table 14: Measured mass of storage tank across three trials.

	Mass Before (kg)	**Mass After (kg)**	**Mass of Air from Compression (kg)**
Trial 1	31.29	32.43	1.04
Trail 2	30.84	31.97	1.04
Trail 3	31.39	32.43	1.04
Average	31.17	32.28	1.04

We graphed the rise in temperature over time and the pressure over time. This helped to verify our initial calculations of the base system. The graphs below show the temperature and pressure graphs for all three trials. This set of preliminary testing showed us that the maximum temperature in the tank is about 410 K. This temperature more closely matches the temperature verified by other compressor manufactures, compared to our isentropic theoretical temperature of about 700 K For the rest of our analyses, we used 410 K as the maximum temperature in the tank.

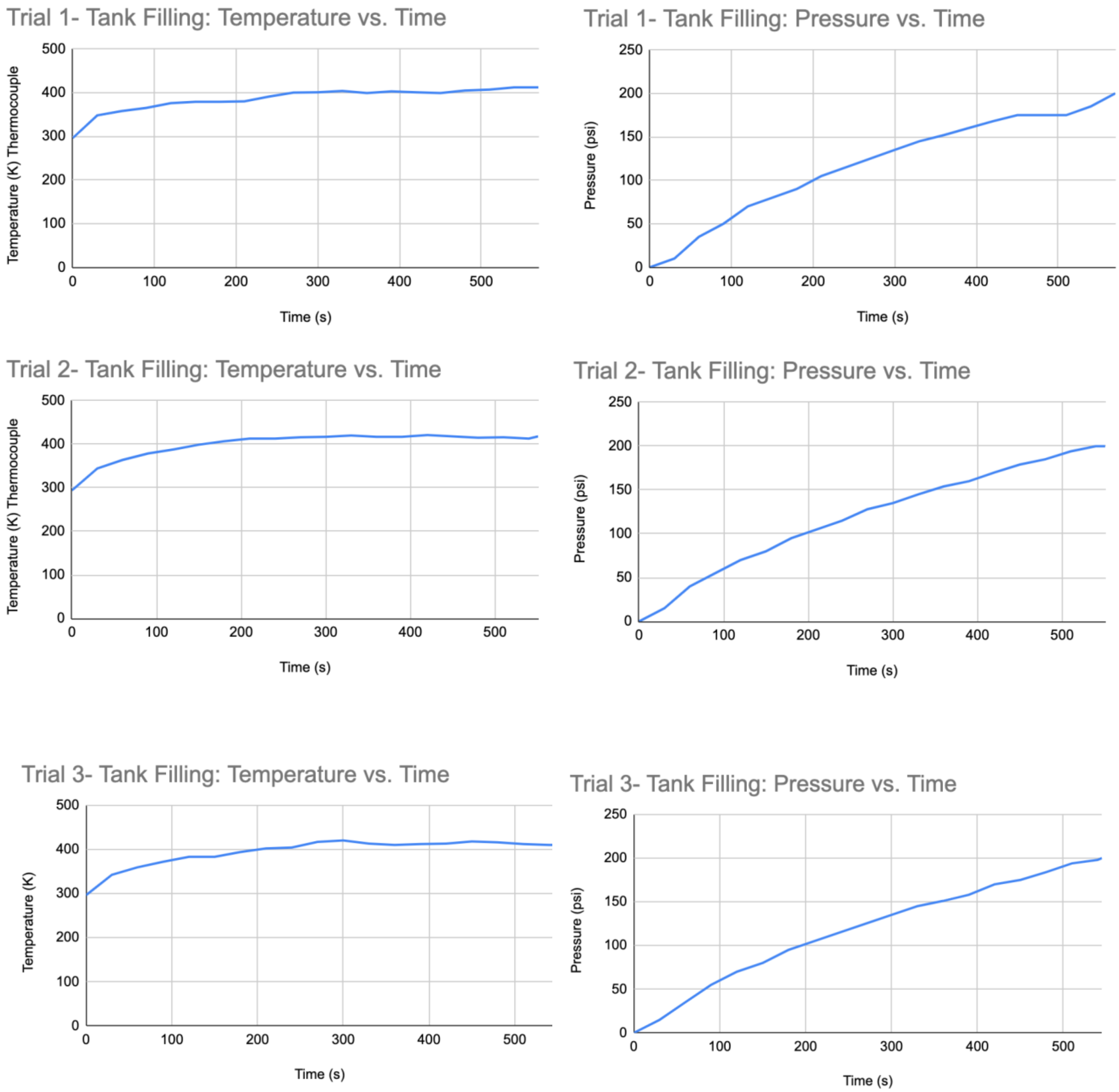

Figure 16: Pressure vs. time and temperature vs. time plots of the three trials.

Below is the graph created for the tank emptying process.

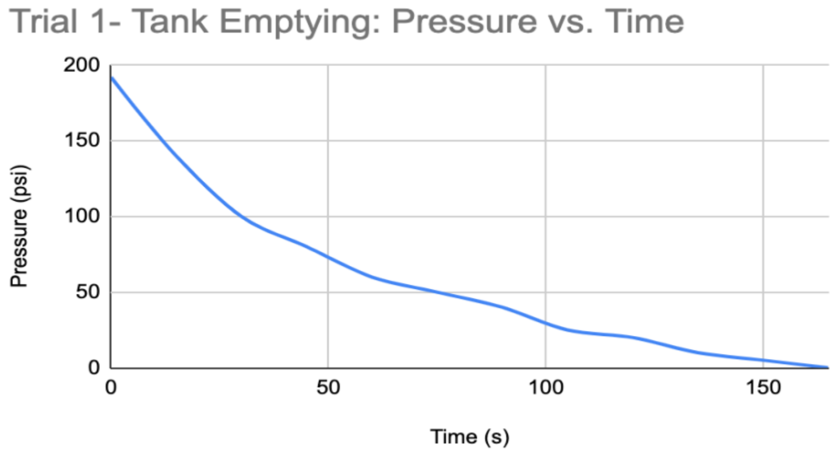

Figure 17: Tank emptying pressure (measured) over time plot.

Below is a table displaying the average temperature of the tank over time.

Table 15: Temperature loss of tank over forty minutes.

Time (min)	**Temp. TOP (C)**	**Temp. BOTTOM (C)**	**Temp. Average (C)**
0	40	34	37
5	41.3	33.1	37.2
10	36.4	31.1	33.75
15	31.1	29.9	30.5
20	31.8	28.8	30.3
25	30.8	28	29.4
30	29.6	27.1	28.35
35	28.9	26.3	27.6
40	27.4	25.9	26.65

The temperature loss observed in the experiment matched the calculated heat loss estimations due to the known wall material, surface area, and wall thickness. This set of testing was only preliminary and allowed our team to see how our preliminary theoretical analysis matched the actual running system.

While emptying the tank, we recorded the voltage every 30 seconds in order to see the voltage drop over time. Tables 16 below show the Voltage vs. Time plots for each of the preliminary trials.

Table 16: Voltage vs. Time Data from Basic System Emptying

Trial 1		
Tank Emptying		
Time (m)	**Time (s)**	**Voltage (volts)**
0.00	0	8.38
0.50	30	7.15
1.00	60	6.08
1.50	90	4.98
2.00	120	3.87
2.50	150	2.86
3.00	180	1.84
3.50	210	1.05
4.00	240	0
Time End: 4:00		

Trial 2		
Tank Emptying		
Time (m)	**Time (s)**	**Voltage (volts)**
0.00	0	8.33
0.50	30	7.16
1.00	60	6.05
1.50	90	4.91
2.00	120	3.88
2.50	150	2.77
3.00	180	1.89
3.50	210	0.98
4.00	240	0
Time End: 3:55		

Trial 3		
Tank Emptying		
Time (m)	**Time (s)**	**Voltage (volts)**
0.00	0	8.93
0.50	30	7.1
1.00	60	5.99
1.50	90	4.91
2.00	120	3.82
2.50	150	2.78
3.00	180	1.81
3.50	210	0.91
4.00	240	0
Time End: 3:53		

This data represents the minimum amount of voltage that our system can generate. We followed the same testing procedure for the final system build with the heat exchanger. The data here allows us to compare how much power our heat exchanger can save in the form of thermal energy.

4.2 Motor/Drill Mounting System

When discussing the collection of data regarding the return power output of the system, we determined that securing the air drill to the electric power generator was necessary to ensure fixed friction and torque quantities in each test. The mounting of the electric generator to the air drill with an automatic triggering system would remove variables and variable human input during testing. To begin we constructed a base for the mounting hardware to be secured. The base consisted of a 2 ft by 1 ft ¾ in thick plywood board. Four 3 in long 2 X 4 woodblocks were fastened vertically to each corner of the base to allow for room under the fixture for mounting purposes. A 2 in diameter hole was cut in the center of the base using a hole saw bit to allow clearance for the handle of the air drill. Two cuts of 4 in 2 x 4 were used as a support structure for the head of the air drill. These were first fastened together with 2 wood screws then secured to the base using 2 more wood screws. Next, a Dremel with a sanding wheel was used to channel out a groove for the head of the drill to rest. A galvanized 1 in steel strap was then used to secure the drill to the raised block. A second 4 in 2 x 4 was used as a raised mount under the electric generator along with a ¾ in thick 3D printed PLA shim. A 3 in diameter galvanized steel strap was used to fasten the electric generator in the required location to allow free spinning of the now connected air drill-electric generator connection. Using a galvanized steel strap, a remote-controlled servo was secured to the base, that actuated the trigger of the air drill. One-inch wood screws were used to secure all steel straps. Lastly, a 3 ft section of ½ in OD rubber air hose was connected to the air drill. A quick-connect fitting was put on the other end. Teflon tape sealed these connections. Figures 18 and 19show the final mounting system.

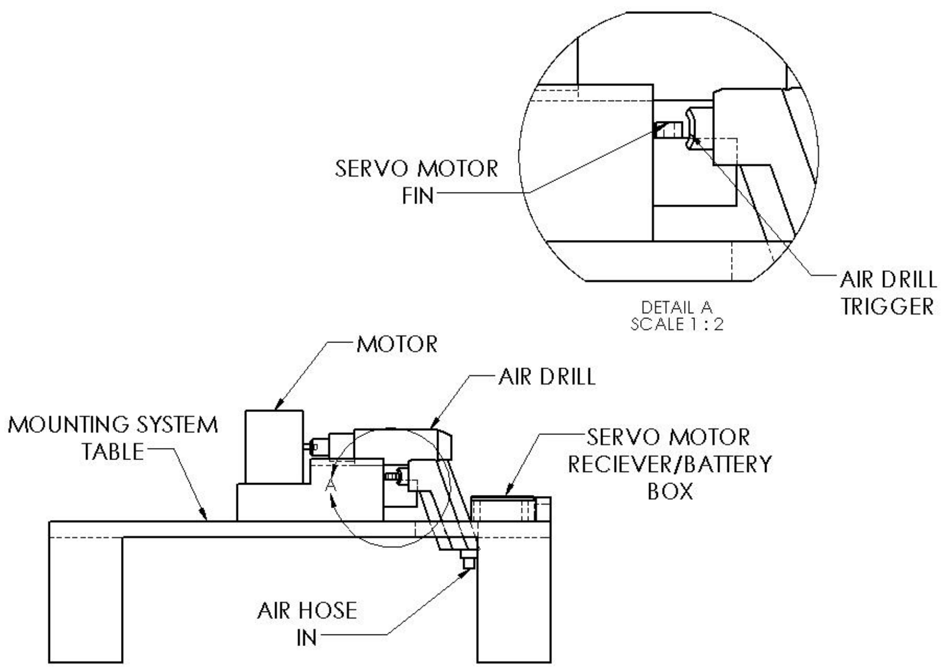

Figure 18: Side view of mounting system

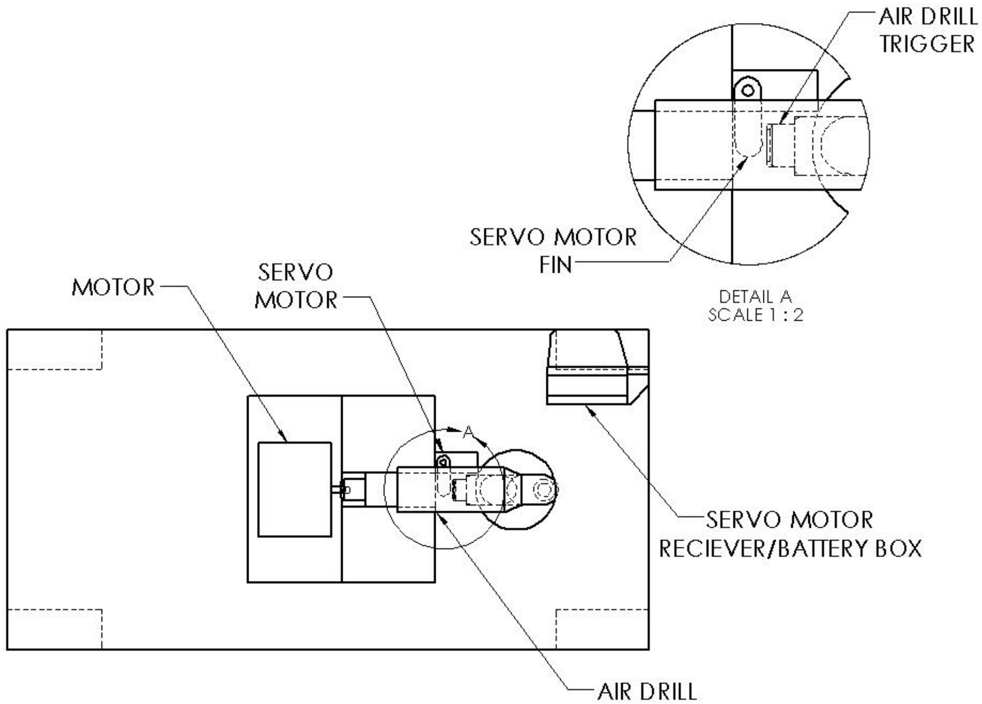

Figure 19: Top view of mounting system

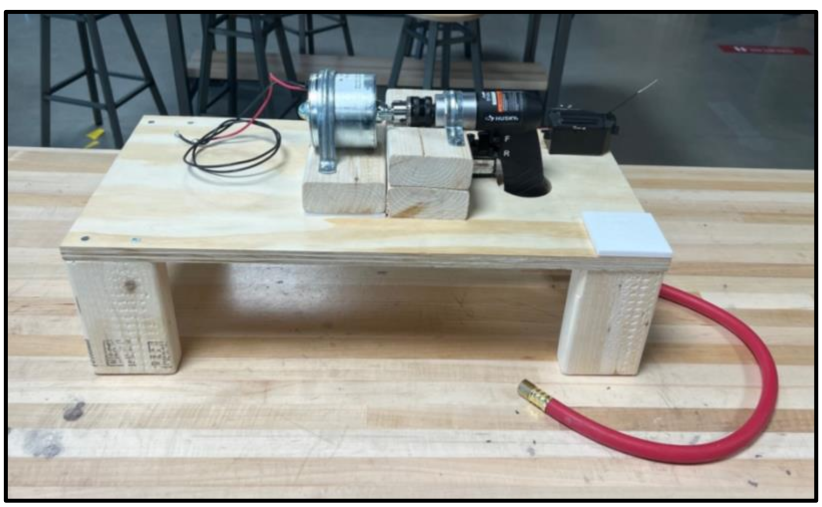

Figure 20: Motor/drill mounting system

4.3 Heat Exchanger Design

4.3.1 Theoretical Analysis

The heat exchanger design is a coiled tube placed in a volume of water. The goal is to remove excess heat during compression to be used as preheating for a hot water tank. Therefore, the ideal maximum temperature of the water would be 327 K.

Using this new final temperature, we calculated the total heat loss using Equation 30 from above, with the only change being the change in temperature.

Plug in values into Equation 33 from above:

$$Q = (0.95\ kg)(1.005\ kJ/kg\ K)(410 - 327\ K)$$

Energy result:

$$\boldsymbol{Q = 79.24\ kJ}$$

$$\boldsymbol{Q = 79240\ J}$$

This is a new Q value, meaning the available energy to transfer from the air to the water with a temperature change of the air from 410 K to 327 K.

Next, we calculated the surface area required for the copper piping, in order to determine the length of the copper piping needed to transfer this energy. The following analysis solves the length of the copper piping required in the heat exchanger.

4.3.2 Copper Piping Selection and Analysis

Energy flow of air through copper pipe:

$$\dot{Q} = \dot{m}(\Delta T)c_{p(air)} \tag{36}$$

Where:

$\dot{Q}$ = heat transfer rate [J/s]

$\dot{m}$= mass flow rate [kg/s]

ΔT = change in temperature of air

$c_{p(air)}$ = specific heat capacity of air [kJ/kg K]

Plug in values:

$$\dot{Q} = (0.002\ kg/s)(410\ K - 327\ K)(1.00\ kJ/kgK)$$

Heat transfer rate result:

$$\dot{Q} = 166\ J/s$$

To solve for the total heat transfer coefficient of heat exchanger, we needed to calculate the convective heat transfer coefficient of air. This analysis is detailed below.

Mass flow rate equation:

$$\dot{m} = \rho V A \tag{37}$$

Where:

$\dot{m}$ = mass flow rate [kg/s]

V=velocity of air [m/s]

ρ=average density of air [kJ/kg^3]

A=Cross sectional area of pipe [m^3]

Rearrange Equation 37 to solve for velocity:

$$V = \frac{\dot{m}}{\rho A} \tag{38}$$

Plug in values:

$$V = \frac{(0.002\ kg/s)}{(7.16\ kg/m^3)(3.17 \times 10^{-5} m^2)}$$

Velocity of air in the pipe result:

$$V = 8.8\ m/s$$

Reynolds Number Equation:

$$Re = \frac{\mathrm{VD}}{\mu} \tag{39}$$

Where:

Re = Reynolds number

V= velocity [m/s]

D_h= Hydraulic diameter [m]

μ = Kinematic viscosity [m^2/s]

Plug in values:

$$Re = \frac{(8.8\ m/s)(0.00635\ m)}{(2.5 \times 10^{-5} m^2)}$$

Reynolds number result:

$$Re = 2032$$

Since this Reynolds number is below 2,300, the flow through the copper pipe is laminar. Since the flow is laminar, the corresponding Nusselt number is a constant 3.66.

Nusselt number equation:

$$Nu = \frac{hD}{k} \tag{40}$$

Rearrange Equation 40 to solve for convective heat transfer coefficient of air:

$$h = \frac{(Nu)(k)}{D}$$

Where:

Nu = Nusselt number

h = convective heat transfer coefficient of air [W/m^2K]

D = Characteristic diameter [m]

k = Conductive heat transfer coefficient [W/m^2K]

Plug in values:

$$h = \frac{(3.66)(0.033\ W/mK)}{(0.00635\ m)}$$

Convective heat transfer coefficient of air result:

$$h = 19.02\ W/m^2K$$

Using this value for the convective heat transfer of air, we next determined the total heat transfer coefficient of the heat exchanger.

Total heat transfer coefficient of the heat exchanger equation:

$$U = \left(\frac{1}{h_{air}} + \frac{s}{k_{copper}} + \frac{1}{h_{water}}\right)^{-1} \tag{41}$$

Where:

h_{air}= convective heat transfer coefficient air [W/m^2K]

h_{water}=convective heat transfer coefficient water [W/m^2K]

s = wall thickness of copper [m]

k=conductive heat transfer coefficient of copper [W/m K]

Plug in values:

$$U = \left(\frac{1}{19.02\ W/m^2K} + \frac{.000762m}{400\ W/mK} + \frac{1}{100\ W/m^2K}\right)^{-1}$$

Total heat transfer coefficient of the heat exchanger result:

$$U = 16.02\ \mathrm{W}/m^2K$$

Rate of heat loss equation:

$$\dot{Q} = SA(\Delta T)U \tag{42}$$

Rearrange Equation X to solve for surface area (SA):

$$SA = \frac{\dot{Q}}{(\Delta T)(U)}$$

Plug in values:

$$SA = \frac{(166\ J/s)}{(410\ K - 327\ K)(16.02\ W/m^2K))}$$

Surface area result:

$$SA = 0.125m^2$$

For the specific copper piping selection, most of the limitations were a result from the current attachments and fittings outlet of the compressor and inlet of the storage tank. The copper piping sizing we selected has a ½-inch outer diameter and a 3/8 inner diameter. The specific dimensions and conversions are presented below in Table 17. These dimensions were used below to calculate the final length of copper piping needed.

Table 17: Copper Piping Dimensions

	Value [in]	Metric conversion [m]
Inner diameter (ID)	0.5	0.0127
Outer diameter (OD)	0.375	0.00952
Inner radius	0.25	0.00635
Outer radius	0.1875	0.00476

Surface area of a cylinder equation:

$$SA = 2\pi(r)(L) + 2\pi(r)^2 \tag{43}$$

In Equation X, the surface area of the top and bottom is negligible because the diameter of the pipe is small compared to the pip length.

The surface area equation reduces to:

$$SA = 2\pi(r)(L) \tag{44}$$

Plug in values to solve for length of cylinder:

$$0.125m^2 = 2\pi(0.004756\ m)(L)$$

Length of copper piping result:

$$\boldsymbol{L = 4.2\ m}$$

This theoretical analysis found that in order to raise the temperature of the water from 293 K (room temperature) to 327 K, we need 4.2 m of copper piping.

4.3.3 Heat Exchanger Build

Next, we built our heat exchanger system. To complete this, we had to change the connection between the air compressor and the tank. We removed the metal pipe that connected the outlet of the compressor to the inlet of the tank. Previous calculations determined the material specifications for this build, and a surface area of 0.125 m^2 was found to be needed to complete all heat transfer between the moving air and water. Originally, our team was going to use ¼ in OD copper tubing resulting in a required length of 6.3 m. Due to fitting compatibility, the copper piping specifications were changed to ½ in OD, resulting in a required length of only 3.13 m.

Copper piping rated to over 1000 PSI was purchased. ½ in compression fittings were used to thread quick connect male NPT fittings to both ends of the heat exchanger. A quick connect coupling fitting was threaded on to the exit pipe of the compressor to connect the compressor outlet to the heat exchanger inlet. Quick connect couplers were threaded onto both ends of the rubber air hose connecting the outlet of the heat exchange to the air tank for storage of the now cooled compressed air. Teflon tape was used to seal all threaded connections. With the required 3.13 meters of coppering piping, a water storage vessel of adequate size was purchased to house the copper coil. This vessel was a 5-gallon cylindrical water cooler designed to retain ice for 2 days.

The next step was to drill holes through the lid of the purchased cooler and remove the spout at the bottom to accommodate the inlet and outlet of the heat exchanger. To seal the outlet at the bottom, we added a combination of JB Weld and Flex Seal spray to both sides of the wall and tested the seal by filling the cooler with water. We worked ½ in OD copper to create a coil slightly smaller than the diameter of the inside of the cooler to ensure that the copper did not touch the plastic inside. Additionally, we added a plastic jug filled with sand in the center of the coil to displace the water, as seen in Figure X.

The original pipe connecting the compressor and the tank was cut to fit the copper piping at the top of the heat exchanger. We covered the piping with fiberglass insulation from the outlet of the compressor to the water level to minimize the heat loss through the pipe. This also helped protect the plastic lid at the points the bare copper would touch. Next, we connected the outlet of the heat exchanger to the inlet of the tank. We used Teflon tape at all these connections for a tighter seal. Because the copper piping cannot be bent at sharp angles, the heat exchanger needed to be elevated. A wooden pedestal was constructed to raise the exchanger. Figure X and Figure X below show the setup of the heat exchanger.

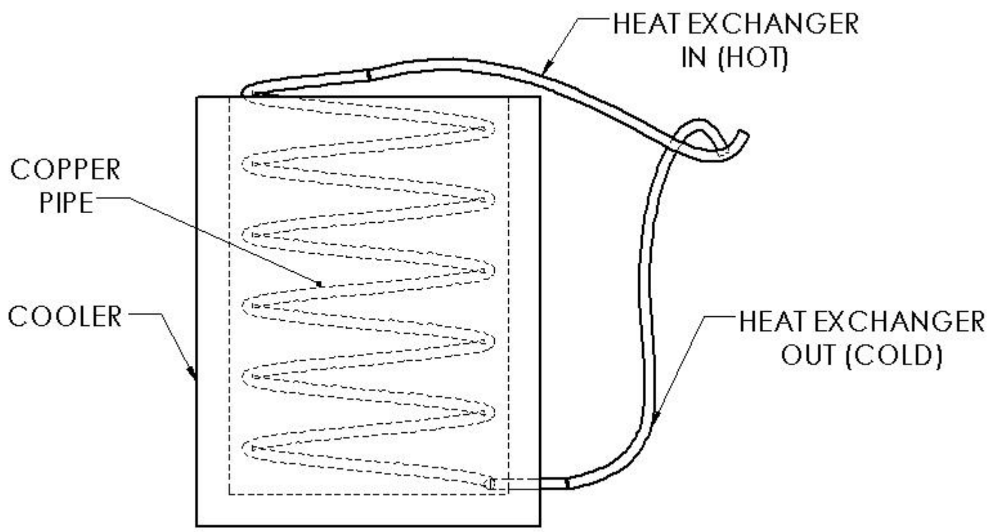

Figure 21: Heat exchanger

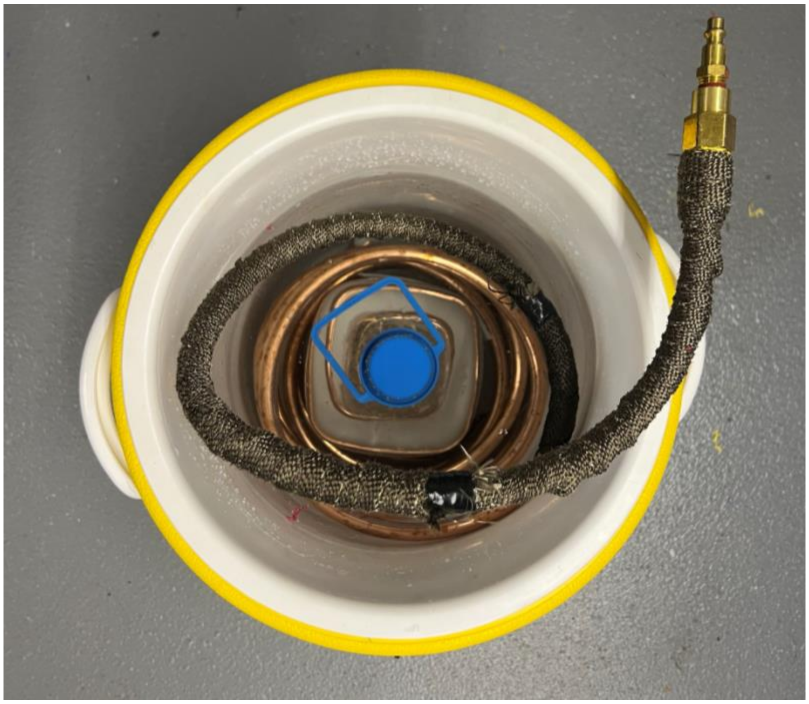

Figure 22: Image of heat exchanger

4.3.4 Final System Build

After analysis of the three proposed systems, we decided to pursue the cogeneration system with an external heat exchanger. This system would allow us to determine the effect of cooling the air before storing it in the tank. It would also allow us to determine the practicality and potential for the heated water in the heat exchanger.

Once the heat exchanger system was built and properly attached as the connection between the air compressor and air tank, we connected the outlet of the air tank to the drill output. To achieve this, a ½ in rubber hose was connected to the outlet regulator of the air tank using a male quick connect fitting. The threaded end of the ½ inch rubber hose was then threaded into the female end of the air drill. Since the rubber air hose was not long, we elevated the mounting system on a table so it was level with the air compressor. The air drill was fitted to the electric generator as described previously. The installed servo is used to actuate the air drill. The positive electrical lead of the electric generator was connected to a 50W 4 Ohm resistor that was then connected to the positive lead of a multimeter. The ground lead of the multimeter was then connected to the ground lead of the electric generator. The multimeter was then used to monitor and record the output voltage of the system.

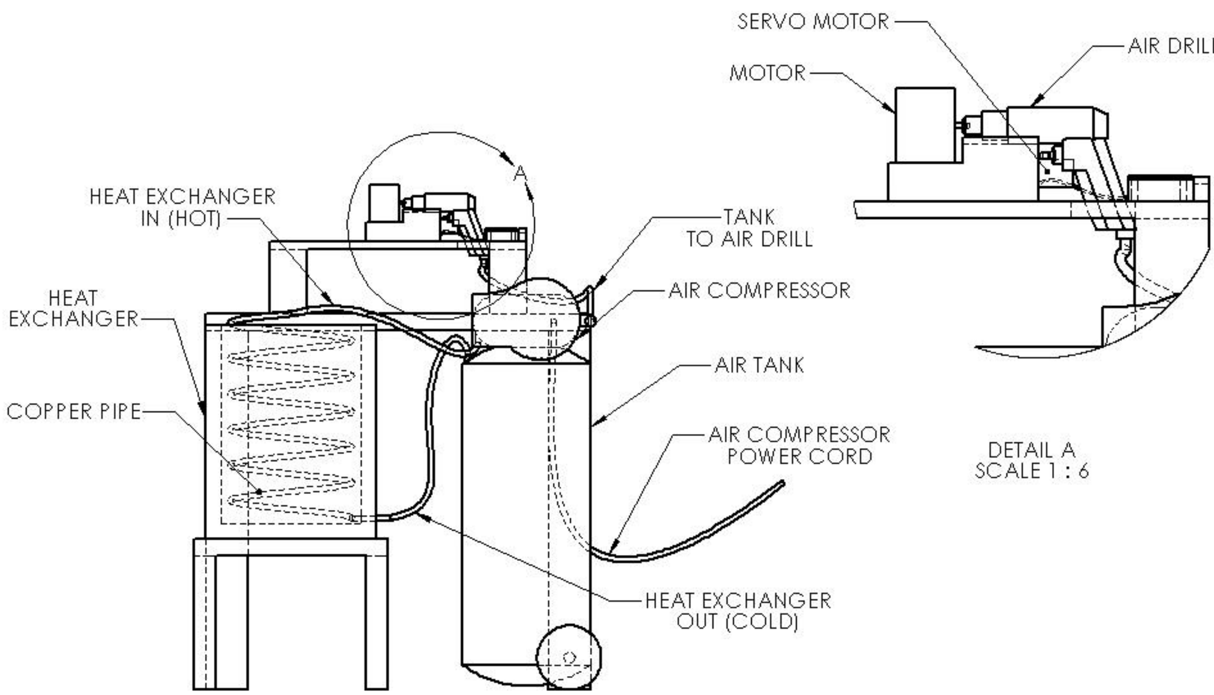

Figure 23: Final system build

Figure 24: Image of final system

Table 18: Final Bill of Materials

Item/Material	**Specs**	**Cost**
Vertical Air Compressor and Tank	20-gal, 200 PSI, 1.3 HP, 4CFM @ 90 PSI	$299.00
Air Drill	2000 RPM at 90 PSI	$54.00
DC Motor from Granger	2,350 RPM 12 volt	$48.05
Copper piping	20 ft. Soft Coil Copper Tubing, 1/2 in Outside Dia., 0.375 in Inside Dia.	$53.38
Cooler	Plastic, 5.0-gal, Beverage Dispenser	$73.45
2' x 2' Plywood	-	$11.49

2" x 4" x 96" Wood Plank	-	$5.48
1-1/2" Pipe Strap (x4)	-	$2.36
3" Pipe Clip (x2)	-	$4.78
2-1/2" Wood Screws (x4)	-	$5.12
1" Wood Screws	-	$1.28
Rubber Lead-In Hose (x2)	3/8" x 30"	$47.96
FNTP Brass Coupler	1/4"	$4.48
MNTP Brass Coupler	1/4"	$3.98
MIP Brass Adapter (x2)	1/2"	$16.90
FIP Brass Reducer (x2)	1/2"	$15.14
FNTP Universal Brass Coupler (x2)	1/4"	$8.96
Replacement Compressor Tube Outlet	C201H TYP2 Service	$18.48
TOTAL SPENT		**$674.29**
Maximum Budget		**$1,250.00**

4.3.5 Electrical Impedance

To maximize the power out of our system, we had to choose the correct resistor to use in series with our load. Following the Maximum Power Transfer Theorem [29], we needed to equal the impedance of our system to the current created by the generator during power creation. From measuring the resistance across our generator, we found that the system had 1 ohm of resistance to start with. To provide equivalent impedance, our team wanted to select a resistor with the value closest to 1ohm, while also having a power rating high enough so it wouldn't burn under the current. We settled on using a 4ohm resistor, rated for 50 W of power. Using these numbers, we were able to calculate what the maximum power out of the system could reach, assuming we used the correct value resistor. While calculating the maximum power, we also needed to justify our choice in resistor. Following Ohm's Law, presented in Equation 41, we calculated the current of the system in amperes.

Ohm’s Law Equation:

$$I = \frac{V_s}{R_s + R_L} \tag{45}$$

Where:

I = Current (A)

V_S = Voltage of System (V)

R_S = Resistance of System (Ohms)

R_L = Load Resistance (Ohms)

For the justification of our selected resistor, we calculated the current using 0.25ohms, 0.5 ohms, 1 ohm, 4 ohms, and 6 ohms. These values gave us a range of power wattages that can prove the Maximum Power Transfer Theorem. The tables showing the current values for each trial can be found in Tables 24. Having solved for the current, we could then solve for the power using the following equation:

$$P = I^2 \cdot R_L \tag{46}$$

Where:

P = Power (W)

I = Current (A)

R_L = Load Resistance

The final power out values for each system using each resistance value can be found in Tables 25.

The tables show that the power generated maxes out when the load resistance is 1 ohm, that aligns with both our prediction and the Max Power Transfer Theorem. Figures 24-26 show the highest power out compared to resistance values. The graphs clearly show the peak of the power coming at 1 ohm. While our team was unable to find a 1ohm resistor that could handle a high-power wattage, we were able to theoretically show what the max would be using the correct resistance.

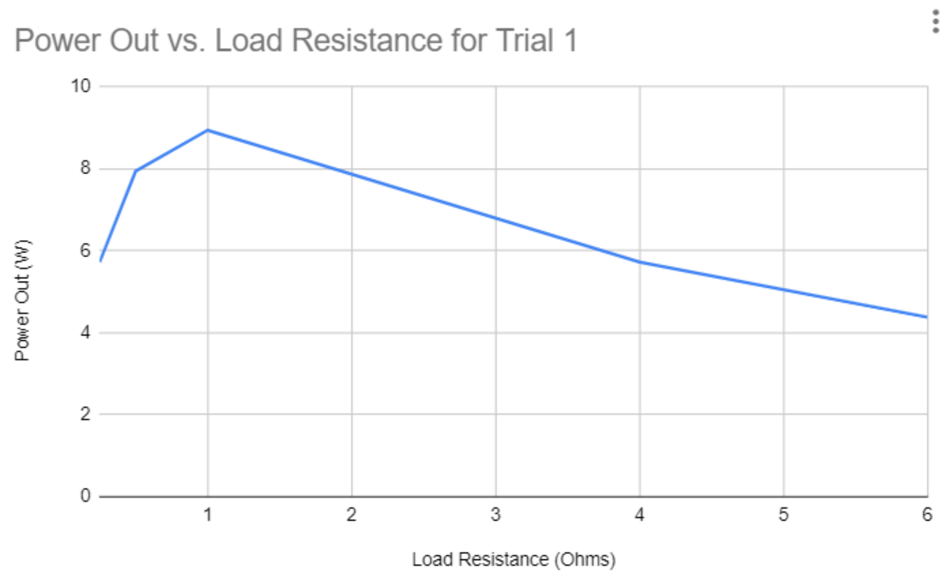

Figure 24: Power Out vs. Load Resistance – Trial 1

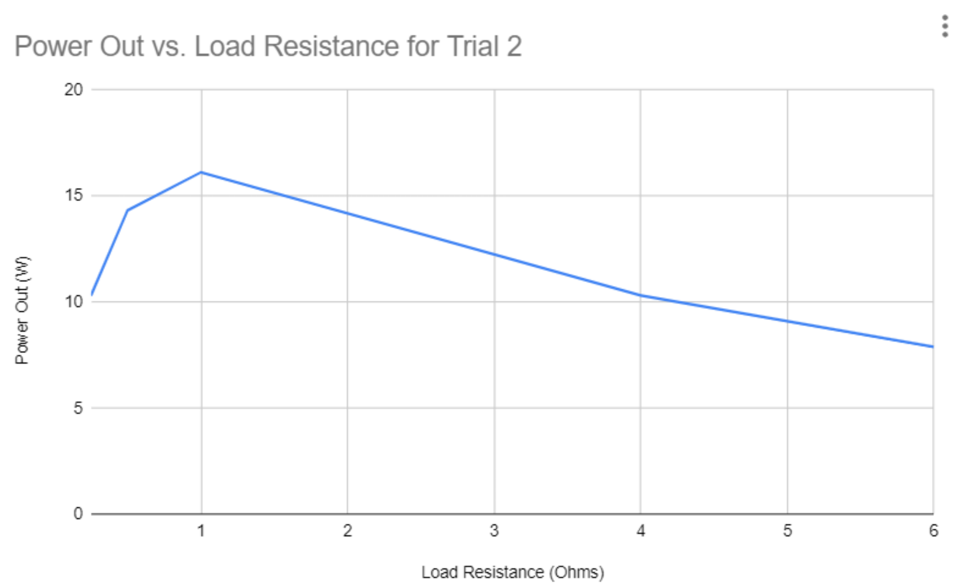

Figure 25: Power Out vs. Load Resistance – Trial 2

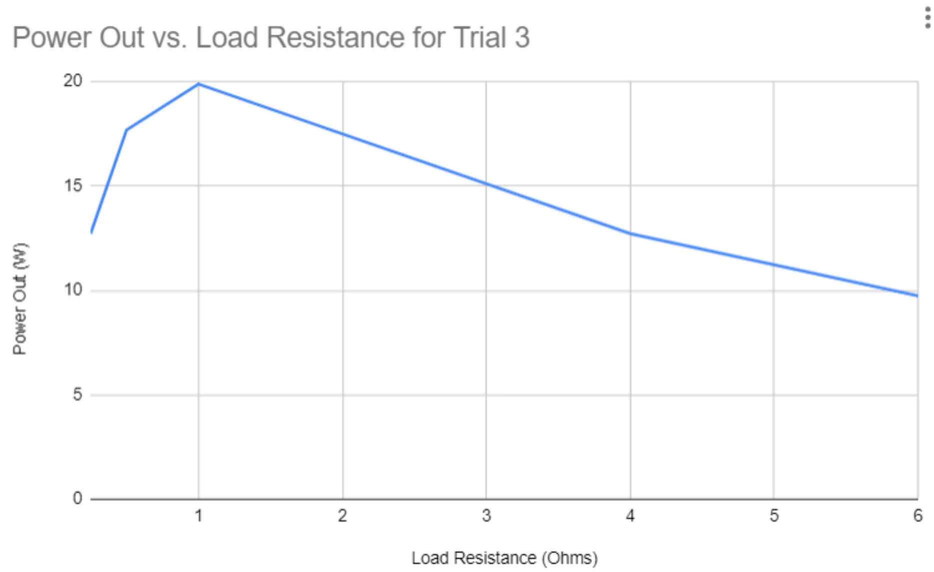

Figure 26: Power Out vs. Load Resistance – Trial 3

4.3.6 Final System Testing Procedure

To begin testing the system was arranged into its operational structure, the heat exchanger was filled with 10 L of room temperature water. The heat exchanger was then placed on the levelling table that raised it to the proper height for connection to the compressor outlet. The heat exchanger outlet was then connected to the air tank using the rubber hose. The 3 ft long ½ in rubber hose was then connected to the output regulator of the air tank. The regulator was opened completely to allow for 1379 kPag (200 psig) air flow. The FLIR thermal imaging camera thermocouple attachment was then used to measure the starting temperature of the water. The compressor was then powered on, and temperature measurements of the water were taken in 60 second intervals. The time to fill to 1379 kPag (200 psig) was recorded as well. The multimeter was then powered on and set to measure volts. The servo motor and remote were powered on as well. The servo was then moved, actuating the air drill allowing complete continuous emptying of the air tank. Instantaneous voltage was recorded every 30 seconds. Total emptying time was recorded as well.

5.0 Results and Analysis

5.1 Heat Exchanger Results

The results from entire system testing are presented below.

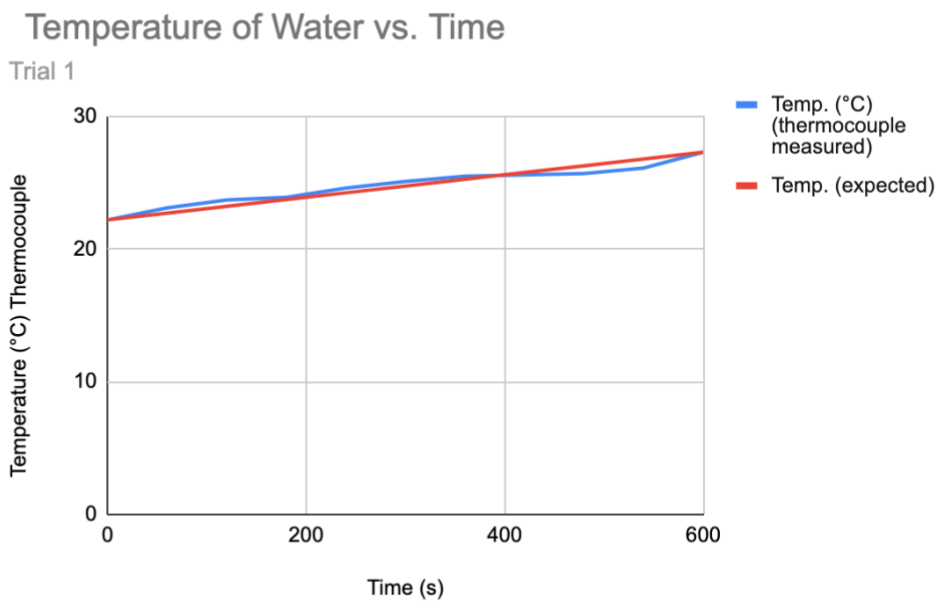

Figure 27: Temperature of Water vs. Time- Trial 1 Results

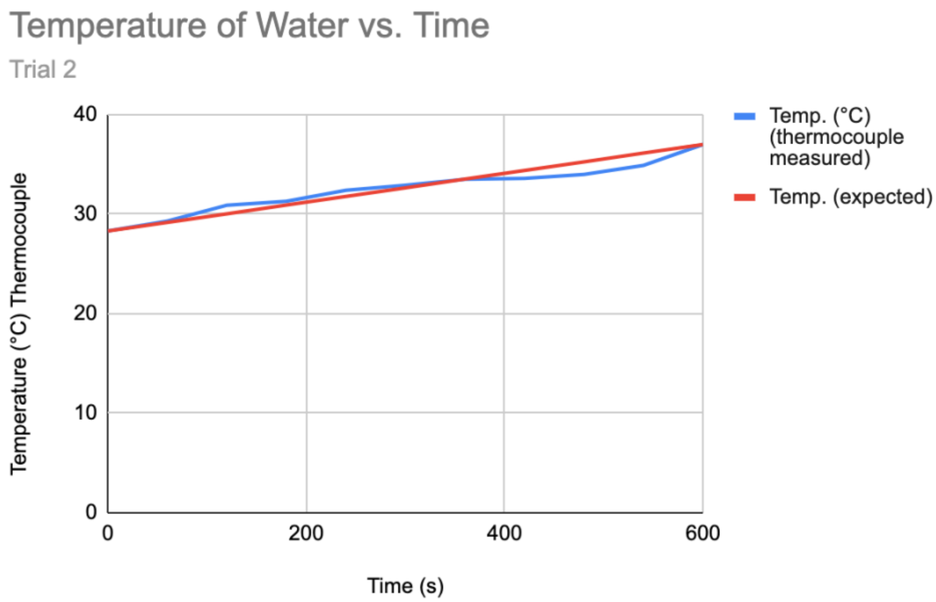

Figure 28: Temperature of Water vs. Time- Trial 2 Results

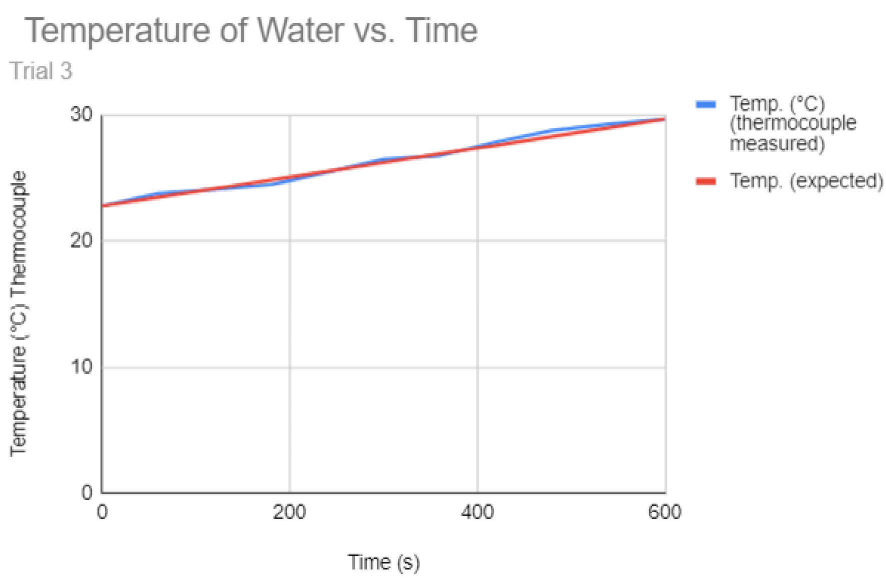

Figure 29: Temperature of Water vs. Time- Trial 3 Results

Table 1919: Heat Exchanger Water Temperature Results Summary

Trial	**Start temp °C**	**End temp °C**	**Change in temp. °C**
1	22.2	27.3	5.1
2	28.3	37.0	8.7
3	23.2	28.9	5.7
Average	*24.6*	*31.1*	*6.5*

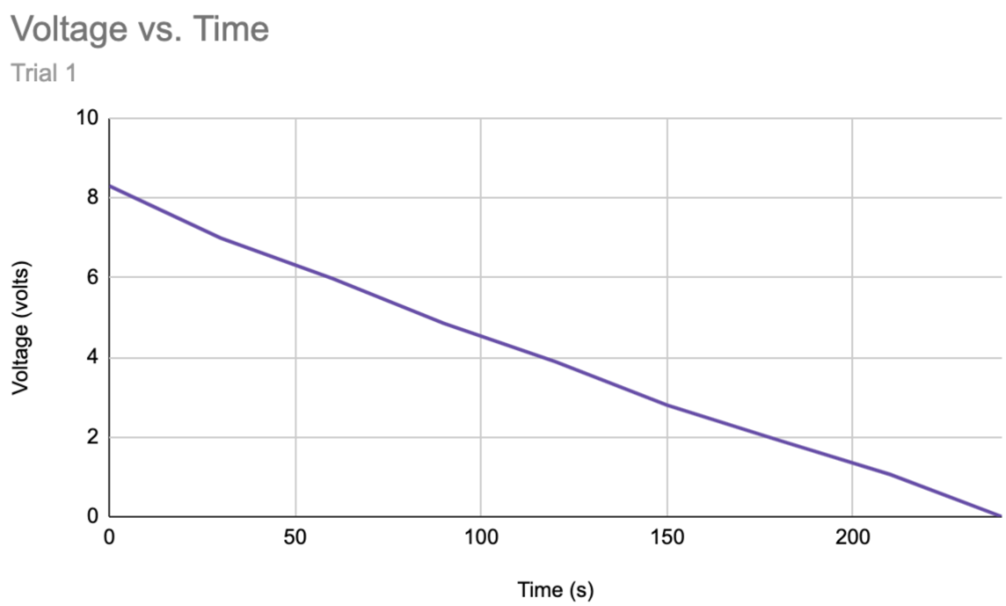

Figure 30: Voltage vs. Time- Trial 1 Results

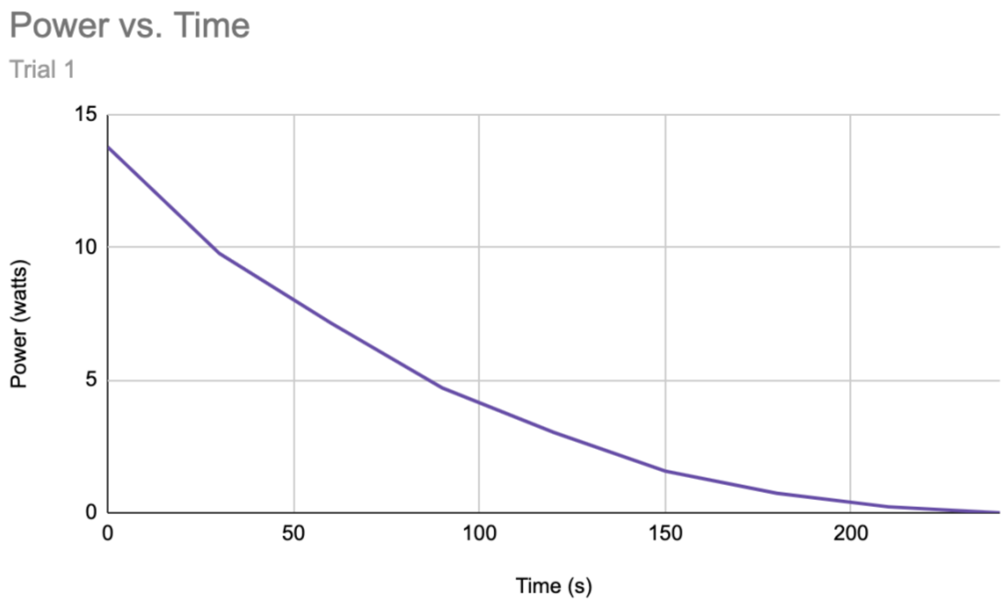

Figure 31: Power vs. Time- Trial 1 Results

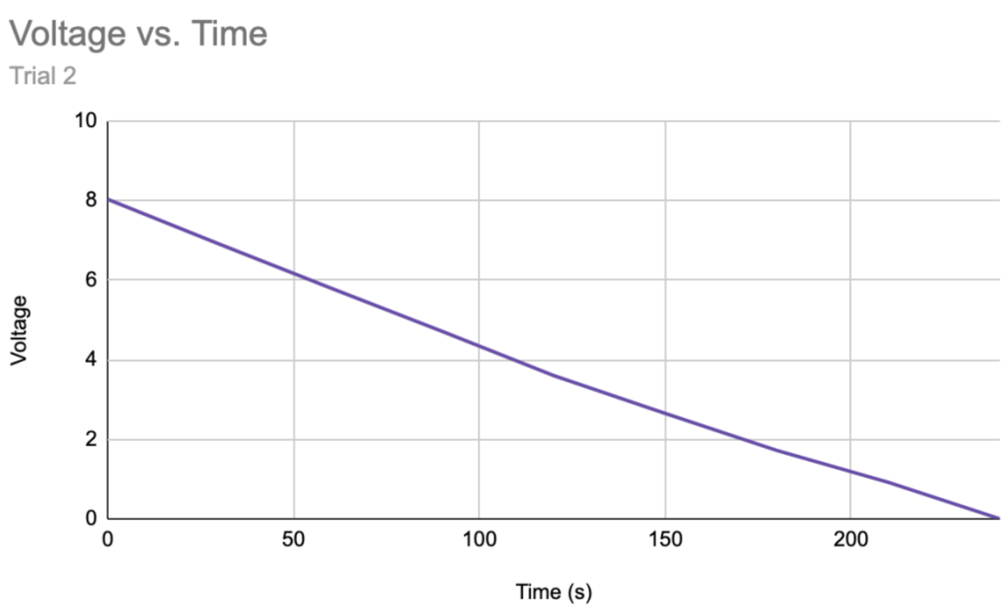

Figure 32: Voltage vs. Time- Trial 2 Results

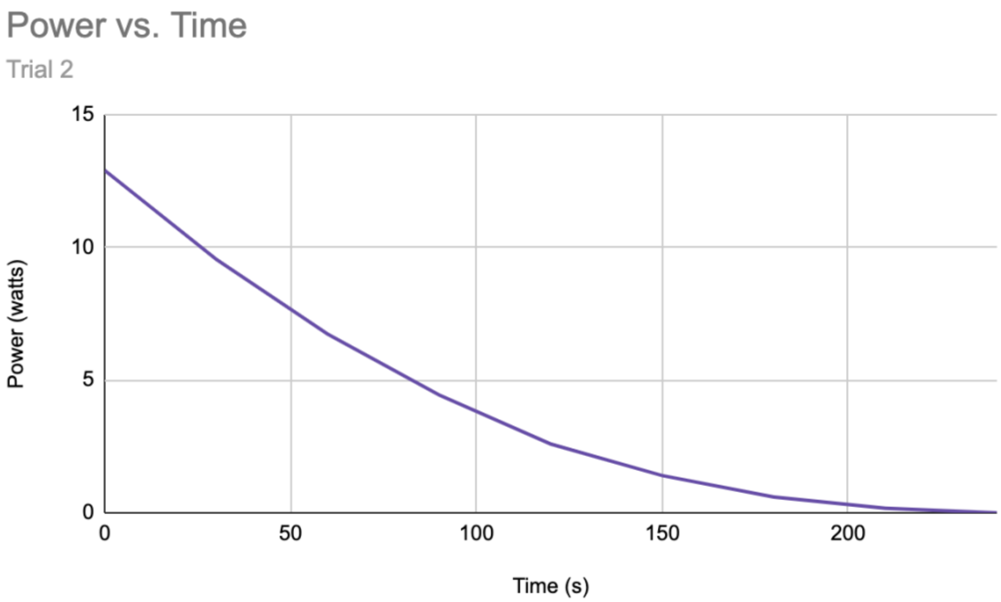

Figure 33: Power vs. Time- Trial 2 Results

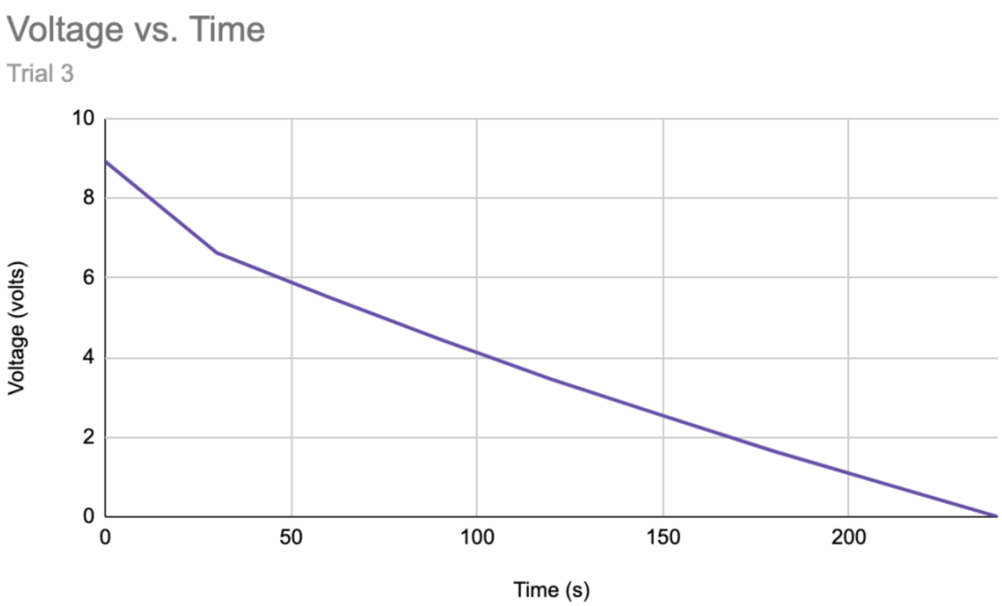

Figure 34: Voltage vs. Time- Trial 3 Results

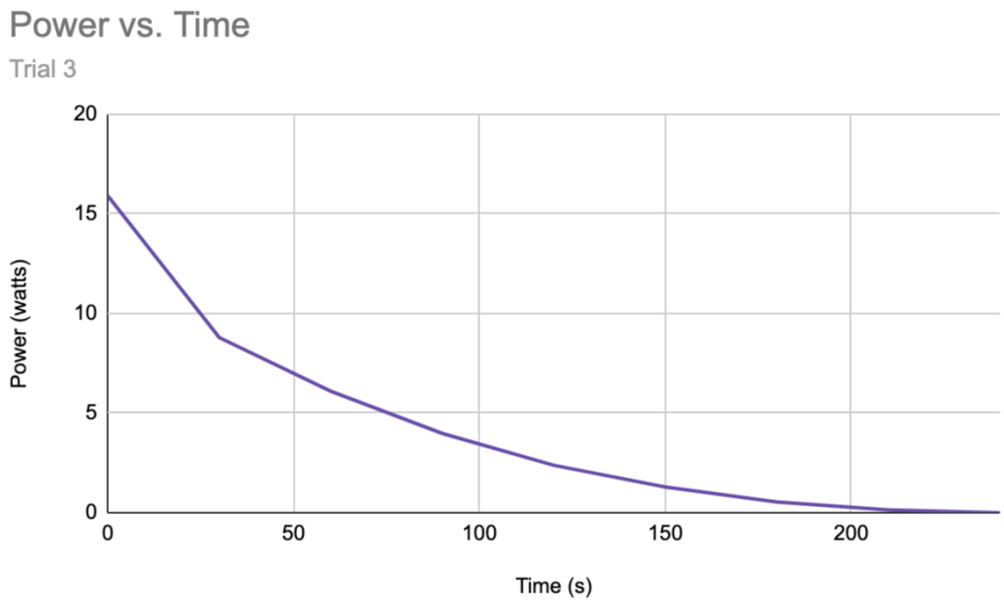

Figure 35: Power vs. Time- Trial 3 Results

Energy Return with Heat Exchanger

Compressor Energy Use:

$$Energy = Motor\ Power(kw) * Run\ Time(s) \tag{47}$$

Plug in values

$$Q = 0.9694(kJ/s) \times 600\ (s)$$

Compressor energy result:

$$Q = 581.64\ kJ$$

581.64 kJ the amount of energy used to fill the 20-gallon air tank to 1379 kPag (200 psig) using the 0.9694 kw motor.

Turbine Driven Electric Generator Energy Production

Average output power output from turbine = 4.89 J/s

Average run time of turbine = 210 seconds

$$Q = 4.89\frac{J}{s} * 210 \text{ seconds}$$

Q = 1.026 KJ

This is the amount of electrical energy produced by the turbine driven electrical generator.

Heat Energy Extracted and Stored in Heat Exchanger

$$Q = mc\,\Delta T \tag{48}$$

Q= (9.97 kg) * (4179 J/kg*k) * (6.5 k)

Q= 270.8 KJ

Heat + electrical energy /total of 580 KJ

5.2 Discussion

After comparing the data from the preliminary test results and the heat exchanger test results, our team was disappointed. At first glance, it seemed like there was no significant change in the run time or maximum voltages. The side-by-side comparison of the average voltages of both systems can be found in Table 20 below. The difference in average run time was 4 seconds, this was expected as more total air mass can be stored in the tank if cooled, as the air density is increased. If you compare the two systems, the average output voltage for the basic system is slightly higher than the average output voltage for the added heat exchanger configuration at each 30 second time marker.

Table 20: The average voltage of the preliminary tests vs. heat exchanger tests

Time (Seconds)	**Preliminary Trials (Volts)**	**Heat Exchanger Trials (Volts)**
0	8.55	8.42
30	7.14	6.84
60	6.04	5.77
90	4.93	4.67
120	3.86	3.65
150	2.80	2.66
180	1.85	1.76
210	0.98	0.93
240	0.00	0.00
	Average Time: 3:56	Average Time: 4:00

The goal of this project was to find a way to capture the heat loss of the system and turn it into usable energy. Through our calculations, we were certain that our heat exchanger should be working with around an 80% efficiency. We took a closer look at the one value that was different in each test, the temperature of the water and the heat exchanger, and our team found that almost all the thermal energy we were missing was being stored in the water.

Within our system, there is roughly 300 kJ of energy going into the compressor, however we are only seeing about 1kJ out at the drill. Most of this energy is what would be lost as thermal energy, and released in the form of heat, vibration, and sound around the system. Based on our calculations, our heat exchanger should be capturing some of that heat energy. By accessing the small volume of water (roughly 10 liters) that we used during testing, we found that the remaining ~299kJ are used to raise the temperature of that water up an average of 6.5 °C.

Simply due to the volume of water we chose and the pressure limit of the compressor, the excess energy going into the water raises it to barely a useful temperature. While our system doesn't convert the saved energy into something useful, it is still what our team had initially set out to do: capture the excess thermal energy as it leaves the system. While at the small scale of our system the energy capture seems insignificant, this system could easily be scaled to be more useful and more realistic for a real-world application. The storage vessel size and pressure that was used in our experiment was very small in comparison to current compressed air energy storage applications. As the pressure of compressed air increases the thermal energy associated with the compression cycle will increase greatly. This larger quantity of thermal energy has many more practical applications. Some suggestions for how this system could be modified to be more useful and realistic are outlined in Section 6.1 below.

6.0 Conclusion and Recommendations

6.1 Recommendations for Future Work

Throughout the duration of this project, our design for the CAES system has taken various different forms, many of which could be achievable within the three seven-week terms with proper planning. Our final heat exchanger system design was a product of many iterations resulting from various challenges. During the proposal stage of this project, we had three main designs of how the system could run: as a cogeneration system, as an insulated storage system, and as an energy storage system with a heat exchanger.

The simplest of the three was the insulated storage system. Our team did theoretical calculations for the amount of fiberglass insulation needed to keep all the thermal energy within the system during compression, as shown in section 4.2. However, due to the amount of insulation needed we decided not to run an insulated system test due to its impracticality. In the future, more research could be done on alternative insulation materials that have a higher R-value than fiberglass and would require much less material.

Our second design was a cogeneration system which is what we ended up building. The design and building process is outlined in section 4. This system design was the one we found most attainable with the amount of planning time we had, and the budget given. This system also allowed us to approximate the amount of thermal energy generated during compression and display how much could be saved using a basic shell and tube heat exchanger design. One of our goals that was not achieved due to lack of time was maximizing voltage output. This could have been done in many ways such as using copper piping with a larger diameter, fully insulating the water tank, or fully insulating any piping not submerged in water. There are many other ways to achieve a greater voltage output that our team has not yet considered that could be explored further.

While the last design is the most complicated, costly, and time consuming, it also offers the greatest amount of potential. This system requires a strong design of a heat exchanger, the incorporation of a phase change material, and the reintroduction of the removed heat back into the system. Our team incorporated this into our original design, researching different phase change materials (PCMs). We had planned to design a heat exchanger around the material we chose. In the early stages of design, our team settled on carbon-16 paraffin wax for the phase change material. Since we realized that this design was not feasible early on, we did not do much further research or theoretical calculations. So, more research and testing could be done to further support the potential of PCMs.

As for the system we were able to build, there were a few choices we made for convenience that could be changed for other trials that would result in different results. All of the parts that we used were what we had available to us at local hardware stores but not specifically designed for the purposes we used them for. For example, the Husky drill we used to convert the air energy into rotational energy was never meant to be used as a generator. Our choice to use an air drill as opposed to a generator that was made specifically for compressed air added more friction into our system. If this system could be remade with higher quality parts designed for their use, perhaps different results could have been achieved.

Another large change that our current system could undergo is the way we incorporated water into our heat exchanger. As discussed in section 5, most of the energy extracted by our heat exchanger was stored in water. The heat exchanger held roughly 10 liters of water which we were able to raise roughly 4 degrees Celsius. Using this ratio of pressure to water, the energy extracted isn't enough to be useable. A few changes that could be made are shrinking the volume of the water held in the heat exchanger, using a larger air tank, and raising the pressure the air tank can hold. If the volume of water in our heat exchanger were to be cut in half, we would have been able to raise the temperature to a useable degree, which would result in a more efficient cogeneration system. However, we believe that the best fix would be to increase the pressure the in the system in order to harness the most power.

6.2 Project Intent and Impact

The purpose of this MQP was to begin research on CAES system usage for smaller real-world applications such as generating energy for a household. Because research on small scale CAES systems is in the early stages, we decided to experimentally show that a micro-CAES system could be reasonably designed and built. Our team's main goal was to design and build a fully working model and use our test results to approximate how much space and resources would be required for the implementation of CAES storage in a household. Given that we had a limited amount of time, resources, and space, we settled on a smaller, table-top-sized system. Although we designed our system in mind to power a small house, CAES has the potential to be used as a greener source of energy storage and with wider applications. Our team has found that CAES is more expensive when it is added to an existing energy system, however costs can be reduced if household generation systems are built specifically in conjunction with CAES systems. Introducing CAES systems for specific buildings is the first step in working towards a fully independent system and towards more heavily relying on green energy.

6.3 Conclusions

All in all, our team is relatively pleased with the results of this project. While our initial plan for this project took multiple forms, our end model became the product of our past ideas. Within the 21 weeks working on the project, our team accomplished our most basic goal: to construct a physical, working model of our system. Our team started out very ambitious, wanting to build multiple iterations of the system and complicated designs. After completing the project, we realize that it would not be feasible to complete every one of these in the amount of time we were given, so we feel accomplished in being able to produce the system we did. Even though we ran into many complications along the way, we were still able to produce a project that we are confident in and proud of.

Although a lot of what we wanted to accomplish within this project became theoretical, the ability to scale up our system and change different parts of it to produce different results proves that there is much potential for CAES systems in the future. We would love to see this project continued and added to future projects. Confidently, our team can conclude that there is a wide range of potential for compressed air storage in the future, both on a smaller and larger scale. CAES provides an alternative option of greener, more cost-effective energy that can be altered to fit a variety of different applications.

Appendix A: Tank Filling and Emptying Results

Table 21: Tank filling pressure and temperature measurements over time across three trials

	Trial 1		**Trial 2**		**Trial 3**	
Time (s)	**Pressure (psig)**	**Temp. (°C)**	**Pressure (psig)**	**Temp. (°C)**	**Pressure (psig)**	**Temp. (°C)**
0	0	23	0	21.3	0	23.2
30	10	75	15	71.5	15	69.1
60	35	85	40	91.1	35	86.2
90	50	92	55	106	55	98.8
120	70	103	70	115	70	110
150	80	106	80	126	80	110
180	90	90	95	134	95	121
210	105	107	105	140	105	129
240	115	118	115	140	115	131
270	125	127	128	143	125	144
300	135	128	135	144	135	147
330	145	131	145	147	145	140
360	152	126	154	144	151	137
390	160	130	160	144	158	139
420	168	128	170	148	170	140
450	175	126	179	145	175	145
480	175	132	185	142	184	143
510	175	134	194	143	194	139
540	185	139	200	140	198	137
570	200	139	200	140	200	137

Table 22: Tank emptying pressure measurements over time

Time (s)	Trial 1-Pressure (psig)
0	190
5	170
10	155
15	140
20	130
25	120
30	110
35	105
40	95
45	90
50	85
55	80
60	75
70	65
80	55
90	50
100	45
110	40
120	35
135	30
150	25
165	20
180	15
195	10
210	0

Appendix B: Current and Power Results

Table 23: Voltage vs. Time Results

Voltage/Time (V/s)		
Trial 1	*Trial 2*	*Trial 3*
8.30	8.03	8.92
6.99	6.91	6.63
5.98	5.8	5.52
4.85	4.71	4.46
3.89	3.6	3.45
2.80	2.65	2.54
1.92	1.72	1.64
1.06	0.92	0.82
0	0	0

Table 24: Current vs. Resistance

Current (A)	*0.25 ohm*	*Extra Below*
Trial 1	*Trial 2*	*Trial 3*
6.64	6.42	7.14
5.59	5.53	5.30
4.78	4.64	4.42
3.88	3.77	3.57
3.1	2.88	2.76
2.24	2.12	2.03
1.534	1.38	1.31
0.85	0.74	0.66
0	0	0

Current (A)	*.5 ohm*	*Below*
Trial 1	*Trial 2*	*Trial 3*
5.53	5.35	5.95
4.66	4.61	4.42
3.99	3.87	3.68
3.23	3.14	2.97
2.59	2.4	2.3
1.87	1.77	1.69
1.28	1.15	1.09
0.71	0.61	0.55
0	0	0

Current (A)	*1 ohm*	*Match*
Trial 1	*Trial 2*	*Trial 3*
4.15	4.02	4.46
3.50	3.46	3.32
2.99	2.9	2.76
2.43	2.36	2.23
1.95	1.8	1.73
1.40	1.33	1.27

Current (A)	*4 ohm*	*Used*
Trial 1	*Trial 2*	*Trial 3*
1.66	1.6	1.78
1.39	1.38	1.33
1.20	1.16	1.10
0.97	0.94	0.89
0.78	0.72	0.69
0.56	0.53	0.51

0.96	0.86	0.82
0.53	0.46	0.41
0	0	0

0.38	0.34	0.33
0.21	0.184	0.16
0	0	0

Current (A)	*6 ohm*	*Higher*
Trial 1	*Trial 2*	*Trial 3*
1.19	1.15	1.27
0.99	0.99	0.95
0.85	0.83	0.79
0.69	0.67	0.64
0.56	0.51	0.49
0.4	0.38	0.36
0.27	0.25	0.23
0.15	0.13	0.12
0	0	0

Table 25: Power vs. Resistance

Power (W)	*0.25 ohms*	*Extra Below*
Trial 1	*Trial 2*	*Trial 3*
11.02	10.32	12.73
7.82	7.64	7.03
5.72	5.38	4.88
3.76	3.55	3.18
2.42	2.07	1.90
1.25	1.12	1.03
0.59	0.47	0.43
0.18	0.14	0.11
0	0	0

Power (W)	*0.5 ohms*	*Below*
Trial 1	*Trial 2*	*Trial 3*
15.31	14.33	17.68
10.86	10.61	9.77
7.95	7.48	6.77
5.23	4.93	4.42
3.36	2.88	2.65
1.74	1.56	1.43
0.82	0.66	0.59
0.25	0.19	0.15
0	0	0

Power (W)	*1 ohm*	*Match*
Trial 1	*Trial 2*	*Trial 3*
17.22	16.12	19.89
12.22	11.94	10.99
8.94	8.41	7.62
5.88	5.55	4.97
3.78	3.24	2.98

Power (W)	*4 ohms*	*Used*
Trial 1	*Trial 2*	*Trial 3*
11.02	10.32	12.73
7.82	7.64	7.03
5.72	5.38	4.88
3.76	3.55	3.18
2.42	2.07	1.90

1.96	1.76	1.62
0.92	0.74	0.67
0.28	0.21	0.17
0	0	0

1.25	1.12	1.03
0.59	0.47	0.43
0.18	0.14	0.11
0	0	0

Power (W)	*6 ohms*	*Higher*
Trial 1	*Trial 2*	*Trial 3*
8.44	7.89	9.74
5.98	5.85	5.38
4.38	4.12	3.73
2.88	2.7	2.44
1.85	1.59	1.46
0.96	0.86	0.79
0.45	0.36	0.33
0.14	0.10	0.08
0	0	0

References

[1] X. Luo, J. Wang, M. Dooner, and J. Clarke, "Overview of current development in electrical energy storage technologies and the application potential in power system operation," *Applied Energy*, vol. 137, pp. 511–536, 2015.

[2] Environmental and Energy Study Institute (EESI), "Fact sheet: Energy STORAGE (2019)," *EESI*. [Online]. Available: https://www.eesi.org/papers/view/energy-storage-2019. [Accessed: 20-Sep-2021].

[3] Zhang, "The economic benefits of battery energy storage system in Electric Distribution System," *Digital WPI*, 25-Apr-2013. [Online]. Available: https://digital.wpi.edu/concern/etds/cf95jb559?locale=en. [Accessed: 15-Oct-2021].

[4] "Electricity Storage," *EPA*. [Online]. Available: https://www.epa.gov/energy/electricity-storage. [Accessed: 22-Sep-2021].

[5] M. Dooner and J. Wang, "Compressed-air energy storage," *Future Energy*, pp. 279–312, 2020.

[6] "Compressed Air Energy Storage," *PNNL*, 01-Aug-2019. [Online]. Available: https://caes.pnnl.gov/. [Accessed: 22-Sep-2021].

[7] K. De Decker, "Ditch the batteries: Off-grid compressed air energy storage," *Low-Tech Magazine*, 16-May-2018. [Online]. Available: https://www.lowtechmagazine.com/2018/05/ditch-the-batteries-off-the-grid-compressed-air-energy-storage.html. [Accessed: 22-Sep-2021].

[8] D. L. Thomas, "Flywheel energy storage - how does it work?," *AZoM.com*, 14-May-2019. [Online]. Available: https://www.azom.com/article.aspx?ArticleID=17336. [Accessed: 22-Sep-2021].

[9] M. Howitt, "CAES or Batteries?," *Storelectric*, 28-Jun-2021. [Online]. Available: https://www.storelectric.com/caes-or-batteries/. [Accessed: 22-Sep-2021].

[10] “Compressed Air Energy Storage (CAES),” *Compressed Air Energy Storage - Energy Storage | CTCN*. [Online]. Available: https://www.ctc-n.org/technologies/compressed-air-energy-storage-caes. [Accessed: 22-Sep-2021].

[11] “CAES: Thermo-Mechanical Energy Storage: Siemens Energy Global,” *Compressed Air Energy Storage*, 2021. [Online]. Available: https://www.siemens-energy.com/global/en/offerings/storage-solutions/thermo-mechanical-energy-storage/caes.html. [Accessed: 21-Sep-2021].

[12] O. J. Guerra, J. Zhang, J. Eichman, P. Denholm, J. Kurtz, and B.-M. Hodge, “The value of seasonal energy storage technologies for the integration of wind and solar power,” *Energy & Environmental Science*, vol. 13, no. 7, pp. 1909–1922, May 2020.

[13] R. McFarlane, “What is an uninterruptible power supply?,” *SearchDataCenter*, 28-May-2019. [Online]. Available: https://searchdatacenter.techtarget.com/definition/uninterruptible-power-supply. [Accessed: osti21-Sep-2021].

[14] “Transmission upgrade deferral,” *Storage Services and Benefits*, 25-Apr-2020. [Online]. Available: https://engineer-educators.com/topic/transmission-upgrade-deferral/#:~:text=Transmission%20upgrade%20deferral%20involves%20delaying,carrying%20capacity%20(design%20rating). [Accessed: 21-Sep-2021].

[15] “Technology overview,” *APEX CAES*, 27-Mar-2019. [Online]. Available: http://www.apexcaes.com/technology-overview. [Accessed: 22-Sep-2021].

[16] B. Castellani, E. Morini, B. Nastasi, A. Nicolini, and F. Rossi, “Small-scale compressed air energy storage application for Renewable Energy Integration in a listed building,” *Energies*, vol. 11, no. 7, p. 1921, 2018.

[17] “Compressed Air Energy Storage (CAES),” *Energy Storage Association*, 07-Apr-2021. [Online]. Available: https://energystorage.org/why-energy-storage/technologies/compressed-air-energy-storage-caes/. [Accessed: 13-Oct-2021].

[18] T. C. Ling, S. Drissi, and K. H. Mo, “Use of phase change materials in nano-concrete for energy savings,” *Smart Nanoconcretes and Cement-Based Materials*, 24-Jan-2020. [Online]. Available: https://www.sciencedirect.com/science/article/pii/B9780128178546000155. [Accessed: 15-Oct-2021].

[19] P. L. Hendrickson, “Legal and regulatory issues affecting compressed air energy storage,” Legal and regulatory issues affecting compressed air energy storage (Technical Report) | OSTI.GOV, 01-Jul-1981. [Online]. Available: http://www.osti.gov/servlets/purl/6476098.

[20] “Husky 20 gal. 200 psig oil free portable vertical electric air compressor-C202H,” *The Home Depot*, 2021. [Online]. Available: https://www.homedepot.com/p/Husky-20-Gal-200-psig-Oil-Free-Portable-Vertical-Electric-Air-Compressor-C202H/312074157?MERCH=REC-_-searchViewed-_-NA-_-312074157-_-N. [Accessed: 15-Oct-2021].

[21] “Dewalt 3/8 in. Pneumatic reversible drill-DWMT70786,” *The Home Depot*, 2021. [Online]. Available: https://www.homedepot.com/p/DEWALT-3-8-in-Pneumatic-Reversible-Drill-DWMT70786/307280891. [Accessed: 15-Oct-2021].

[22] “DC permanent magnet motor, 1/35 hp, non-standard frame, nameplate rpm 2,350, Voltage 12V DC,” *Grainger*, 2021. [Online]. Available: https://www.grainger.com/product/3LCH7?ef_i. [Accessed: 15-Oct-2021].

[23] “Amazon.com: Olive drab green warm wool fire retardant ...,” *Amazon*, 2021. [Online].Available:https://www.amazon.com/Olive-Green-Retardant-Blanket-Military/dp/B00D1AJVHY. [Accessed: 17-Dec-2021].

[24] S. Wicki and E. G. Hansen, “Clean Energy Storage Technology in the making: An innovation systems perspective on flywheel energy storage,” *Journal of Cleaner Production*, 24-May-2017. [Online]. Available: https://www.sciencedirect.com/science/article/pii/S0959652617310764?via%3Dihub#sec6. [Accessed: 26-Jan-2022].

[25] "Oil-Free Compressor," *Oil free compressors - air guru*. [Online]. Available: https://www.airguru.in/oil-free-compressor.php#:~:text=Normal%20temperatures%20for%20low%20pressure,compressed%20air%20becomes%20very%20hot. [Accessed: 26-Jan-2022].

[26] "Average electric bill for 1 & 2 bedroom apartments: Inspire," *Inspire Clean Energy*, 21-Jul-2021. [Online]. Available: https://www.inspirecleanenergy.com/blog/sustainable-living/average-apartment-electric-bill#:~:text=How%20many%20kWh%20does%20an,20%2D30%20kWh%20a%20day. [Accessed: 26-Jan-2022].

[27] D. Yalanovsky, "Highest R-value water heater insulation blanket," *Home Guides | SF Gate*, 17-Nov-2020. [Online]. Available: https://homeguides.sfgate.com/highest-rvalue-water-heater-insulation-blanket-88200.html. [Accessed: 26-Jan-2022].

[28] "Solids, liquids and gases – thermal conductivities," *Engineering ToolBox*. [Online]. Available: https://www.engineeringtoolbox.com/thermal-conductivity-d_429.html. [Accessed: 26-Jan-2022].

[29] "Maximum Power Transfer Theorem in DC theory," *Basic Electronics Tutorials*, 03-May-2018. [Online]. Available: https://www.electronics-tutorials.ws/dccircuits/dcp_9.html. [Accessed: 01-Mar-2022].